Nagra
Nationale
Genossenschaft
für die Lagerung
radioaktiver Abfälle

Cédra
Société coopérative
nationale
pour l'entreposage
de déchets radioactifs

Cisra
Società cooperativa
nazionale
per l'immagazzinamento
di scorie radioattive

TECHNICAL REPORT 88-41

STRIPA PROJECT

ANNUAL REPORT 1987

JUNE 1988

Parkstrasse 23 5401 Baden/Schweiz Telephon 056/20 55 11

Nagra
Nationale
Genossenschaft
für die Lagerung
radioaktiver Abfälle

Cédra
Société coopérative
nationale
pour l'entreposage
de déchets radioactifs

Cisra
Società cooperativa
nazionale
per l'immagazzinamento
di scorie radioattive

TECHNICAL REPORT 88-41

STRIPA PROJECT

ANNUAL REPORT 1987

JUNE 1988

Parkstrasse 23 5401 Baden/Schweiz Telephon 056/20 55 11

Das Stripa-Projekt ist ein Projekt der Nuklearagentur der OECD. Unter internationaler Beteiligung werden im Rahmen einer 3. Phase dieses Projektes von 1986-1991 Forschungsarbeiten in einem unterirdischen Felslabor in Schweden durchgeführt. Unter Anwendung des in den vorhergehenden Phasen 1 und 2 Gelernten sollen folgende Arbeiten realisiert werden:

- Anwendung verschiedener Felduntersuchungs- und Berechnungsmethoden, um den Wasserfluss und Nuklidtransport in einem unbekannten Felsvolumen des Stripagranites vorherzusagen und anschliessend zu überprüfen
- Evaluation verschiedenster Materialien und Methoden zum Abdichten wasserführender Klüfte im Stripagranit

Seitens der Schweiz beteiligt sich die Nagra an diesen Untersuchungen. Die technischen Berichte aus dem Stripa-Projekt erscheinen gleichzeitig in der NTB-Serie der Nagra.

The Stripa Project is organised as an autonomous project of the Nuclear Energy Agency of the OECD. Over the time period 1986-1991 (Phase 3 of the Project), an international cooperative programme of investigations is being carried out in an underground rock laboratory in Sweden. Building on experience gained in Phases 1 and 2, the following research will be carried out:

- Application of various site characterisation techniques and analysis methods with a view to predicting and validating groundwater flow and nuclide transport in an unexplored volume of Stripa granite
- Verification of the use of different materials and techniques for sealing water-bearing fractures in the Stripa granite

Switzerland is represented in the Stripa Project by Nagra and the Stripa Project technical reports appear in the Nagra NTB series.

Le projet de Stripa est un projet de l'Agence de l'OCDE pour l'Energie Nucléaire. C'est dans le cadre d'une troisième phase de ce projet allant de 1986 à 1991, que des travaux de recherches sont réalisés avec une participation internationale, dans un laboratoire souterrain de Suède. Il s'agit d'effectuer les travaux ci-dessous, en mettant en application ce que l'on a appris au cours des précédentes phases 1 et 2:

- Application de diverses méthodes de recherches sur le terrain et de calcul, pour prévoir puis contrôler l'écoulement de l'eau et le transport des nucléides dans un volume rocheux inconnu du granite de Stripa
- Evaluation des méthodes et des matériaux les plus divers, en vue de colmater des fractures aquifères du granite de Stripa

La Cédra participe à ces recherches pour la Suisse. Les rapports techniques rédigés à propos du projet de Stripa paraissent en même temps dans la série des Rapports Techniques de la Cédra (NTB).

THE STRIPA PROJECT ANNUAL REPORT 1987

The Stripa Project is an international project being performed under the sponsorship of the OECD Nuclear Energy Agency (NEA). The Project concerns research related to the disposal of highly radioactive waste in crystalline rock. The Research and Development Division of the Swedish Nuclear Fuel and Waste Management Company (SKB) has been entrusted with the management of the project, under the direction of representatives from each participating country.

The aim of this report is to inform the OECD Nuclear Energy Agency and the participants in the project about the general progress of work during 1987.

Stockholm

June 1988

CONTENT

1 INTRODUCTION

An autonomous OECD/NEA Project relating to the final disposal of highly radioactive waste from nuclear power generation is currently under way in an abandoned iron ore mine at Stripa in central Sweden. Research is being performed in a granite formation 350 meters below the ground surface. The Stripa project was started in 1980, in co-operation with Canada, Finland, France, Japan, Sweden, Switzerland, and the United States. The first phase of the project, completed in 1985 at a total cost of approximately 47 MSEK, consisted essentially of three parts:

- o hydrogeological and hydrogeochemical investigations in boreholes down to a depth of 1230 metres below the ground surface,
- o tracer migration tests to study radionuclide transport mechanisms in the rock fractures, and
- o large-scale tests of the behaviour of backfill material in deposition holes and tunnels.

The second phase of the Stripa Project, which has also been joined by Spain and the United Kingdom, started in 1983 and is currently scheduled for completion in 1988. The estimated total cost is 65 MSEK. The investigations included in the second phase are:

- o the development of crosshole geophysical and hydraulic methods for the detection and characterization of fracture zones,
- o extended tracer experiments in fractured granite,
- o the sealing of boreholes, a shaft and a tunnel using highly compacted bentonite,
- o hydrogeological characterization of the Stripa site based on data from the Swedish-American co-operative (SAC) project, and
- o isotopic characterization of the origin and geochemical interactions of the Stripa groundwaters.

The formal agreement for an extension of the project into a third phase was signed in 1987. Participating countries in this Phase 3 of the Stripa Project is Canada, Finland, Japan, Sweden, Switzerland, United Kingdom and the United States. The research activities in the third phase of the Stripa Project will be carried out under two headings

- Fracture Flow and Nuclide Transport; and
- Groundwater Flow Path Sealing.

Under the heading fracture flow and nuclide transport the main objectives are:

- to predict groundwater flow and nuclide transport in a specific unexplored volume of the Stripa granite and make a comparison with data from field measurements. The comparison will be made by means of an integrated approach with existing site

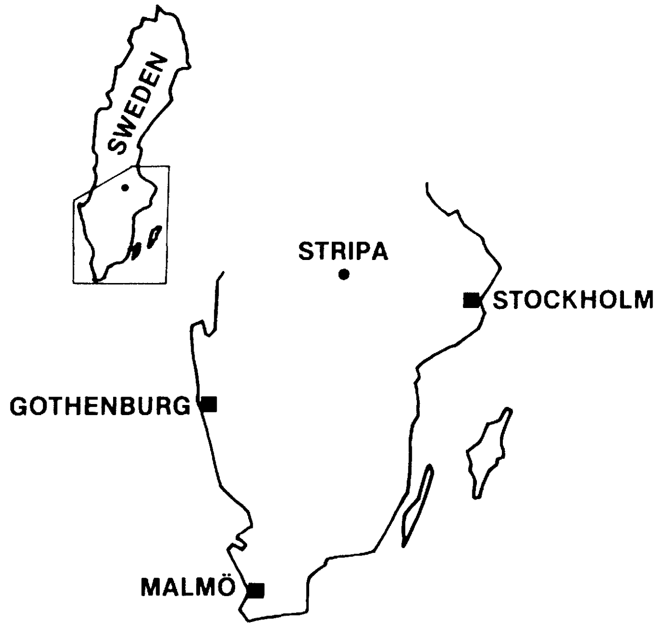

Figure 1-1. The Stripa mine is located approximately 250 km west of Stockholm.

characterization tools and methods, particularly those developed under Phases 1 and 2, this programme is referred to as the "Site Characterization and Validation" programme,

- to continue the development of site assessment methods and strategies and, where found appropriate, apply them in later stages of the integrated site characterization exercise outlined above.

Under the heading groundwater flow path sealing the principal objectives are:

- to identify, select and evaluate sealing substances which promise to possess long-term chemical and mechanical stability; and

- to demonstrate in a pilot test, by use of suitable methods and techniques, the effectiveness of such substances for the long-term sealing of groundwater flow paths in the Stripa granite.

The conditions of participation in the Stripa Project are covered by separate agreements for Phase 1, Phase 2 and Phase 3, although all three phases share the same management structure. The project is jointly funded by the organizations listed below.

Responsibility for supervision of the research programme and for its finance resides with the Joint Technical Committee (JTC). This is composed of representatives from each of the national organizations. It also provides information on the general progress of work to the OECD Steering Committee for Nuclear Energy, through the NEA Committee on Radioactive Waste Management.

Each research activity is assigned to a principal investigator, a scientist with particular expertise in the research field in question. The conception of the experiments, and their realization, are periodically reviewed by a Technical Subgroup (TSG). The sub-group is composed of scientists from the participating countries. It deals with geology, geophysics, hydrogeology, numerical modelling of fracture flow, hydrogeochemistry, rock mechanics, chemical transport and engineered barriers.

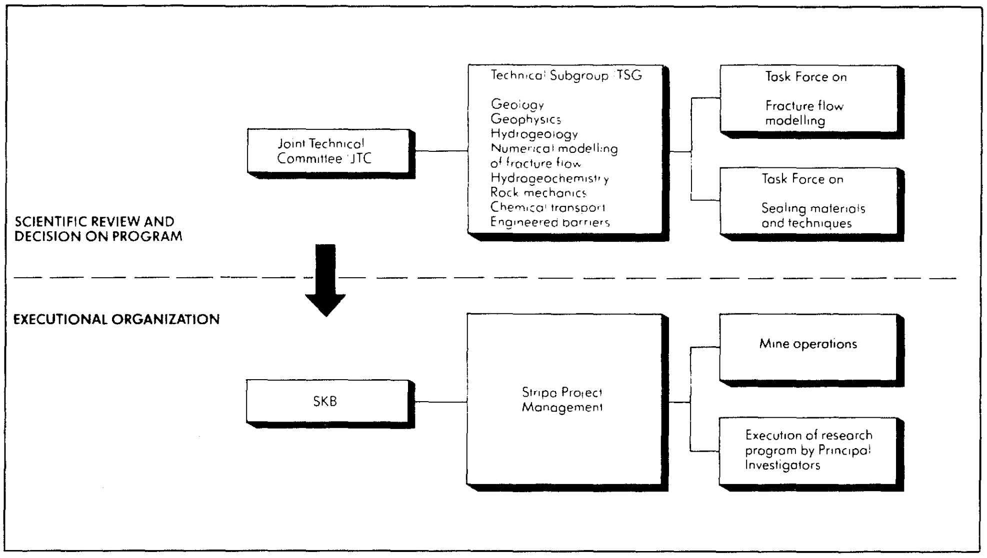

Figure 1-2. Organization of the Stripa Project.

Two "Task Force" groups one on Sealing Materials and Techniques and a second on Fracture Flow Modelling form ad hoc groups to the project. In each of the two groups the participating countries may assign a scientist with particular expertise in the research field considered. The ad hoc groups should report to the TSG on their activities.

As for the "Site Characterization and Validation" programme the project manager is supported by two Scientific Coordinators, John Black of Golders Associates and Olle Ollson of SGAB both with long experience in the Stripa Project. The "Site Characterization and Validation" programme will both in its phase of practical work in the Stripa mine and in the stages of data evaluation and reporting, call for extensive co-ordination between different groups of investigators. A detailed technical knowledge of the work within the programme is then necessary.

The Research and Development Division of the Swedish Nuclear Fuel and Waste Management Company (SKB) acts as the host organization, and provides management for the project. It is responsible for mine operations and for the procurement of equipment and material for experimental work. Meetings of the Joint Technical Committee, the Technical Sub-group, the two Task Force groups, the principal investigators and the project management are held on a regular basis to review the progress of the project.

A representative of the OECD Nuclear Energy Agency takes part in the meetings of the Joint Technical Committee in an advisory capacity. The Nuclear Energy Agency continues to foster the broadest possible participation in this and other projects by its member countries, and ensures co-ordination of the project with its other activities in the field of radioactive waste management.

The following organizations are participating in the Stripa Project:

Canada	Atomic Energy of Canada Ltd (AECL)
Finland	Industrial Power Company Limited (TVO); Ministry of Trade and Industry; Imatra Power Company (IVO)
France (Phase 2 only)	Commissariat á l'Energie Atomique (CEA); Agence Nationale pour la Gestion des Dàchets Radioactifs (ANDRA)
Japan	Power Reactor and Nuclear Fuel Development Corporation (PNC)
Spain (Phase 2 only)	Junta de Energia Nuclear (JEN)
Sweden	Swedish Nuclear Fuel and Waste Management Co
Switzerland	National Co-operative for the Storage of Radioactive Waste (NAGRA)
United Kingdom	Department of the Environment (UK DOE)
United States	Department of Energy (US DOE)

2 GENERAL

2.1 Meetings

The Technical Subgroup met on March 24-25, 1987 in Helsingfors, Finland to review the technical progress of the experiments of Phase 2 as well as to review and discuss the progress of Phase 3 of the Stripa Project. A visit to the Lovisa nuclear power plant and a contruction site for a gas storage was arranged on March 26 in conjunction with the meeting.

A JTC-meeting was held at the OECD Headquarters in Paris, on May 5-6, 1987. The management of the ongoing Stripa Project activities were discussed. The technical and financial status of Phase 2 and Phase 3 of the Stripa Project was also presented. At the meeting a decision was taken to produce a new Stripa brochure as well as a new Stripa film. It was also decided to arrange a Stripa Symposium in September of 1989.

The Task Force on Sealing Materials and Techniques met twice to discuss and review the technical progress of the Rock Sealing programme.

Notes from all meetings have been distributed separately.

3 PHASE 2

3.1 CROSSHOLE TECHNIQUES FOR THE DETECTION AND CHARACTERIZATION OF FRACTURE ZONES

The principal investigator for this project has been Dr. Olle Olsson, Swedish Geological Co., Uppsala Sweden. Jörgen Pihl, Swedish National Defense Research Institute (FOA), Stockholm, Sweden, and Calin Cosma, Vibrometric OY, Helsinki, Finland, have been responsible for the seismic subprogramme. John Black, British Geological Survey, Keyworth, United Kingdom, have been responsible for the hydraulics subprogramme.

3.1.1 Introduction

The objective of the Crosshole Program was to develop methods which could yield information on the suitability of a rock mass for final disposal of radioactive wastes. An important criterion was that the methods employed should be nondestructive, i.e. an investigation should only require a few boreholes. The main reason for limiting the number of holes during a site investigation is that the investigation holes themselves might provide significant transport paths for the groundwater. In the development of the investigation methods, effort has concentrated on the identification and characterization of fracture zones, which are considered to be the most important transport paths. A detailed study of the presence, character, and transport capacity of individual fractures has not been within the scope of the current program. The Crosshole programme has comprised the development of borehole radar, borehole seismic, and hydraulic testing methods. These methods provide data on the electric, elastic, and hydraulic properties of the rock. For each of these methods new equipment has been developed, field tests have been performed, interpretation techniques developed and tested on the obtained data. Finally, the results obtained with the different methods have been compared.

3.1.2 Geophysical Methods

A major effort of the Crosshole program has been the development of borehole radar and seismic methods. An unique aspect of these methods compared to most other site characterization techniques is that they are based on wave propagation through rock. Investigation methods based on wave propagation have the advantage that they combine high resolution with large range. The resolution that can be obtained is on the order of half a wavelength while the range is determined by the attenuation of the waves. Wave methods are useful if the waves can propagate at least a few wavelengths through the rock. If that is the case they can provide high resolution information at considerable distances from the boreholes.

The borehole radar has been used in three different measuring modes; single hole reflection, crosshole reflection, and crosshole tomography. These different modes of measurement provide different types of data. The reflection modes basically provide geometric data on features located at a distance from the borehole, in addition the strength of the reflexes give information on the contrast in electrical properties. The reflection method has high resolution and is sensitive even to features with low contrast in properties. The information obtained from a single-hole measurement is cylindrically symmetric with respect to the hole. This implies that the orientation of a fracture zone can not be obtained from measurement in one borehole only. A method has been devised where absolute orientation of fracture zones is obtained by combining single-hole reflection data from a few adjacent holes. Similar methods for analysis of crosshole reflection data have also been developed and found efficient.

The interpretation of the radar results obtained from the three different modes of measurement have yielded a consistent description of the fracture zones at the Crosshole site. The radar has given a resolution of one to three metres. The probing range obtained in the Stripa granite is approximately 100 m in the single-hole mode and 200 to 300 m in the crosshole mode.

The seismic method has mainly been applied in the crosshole tomography mode. Here variations in the arrival time of the direct wave between transmitter and receiver is studied. If a sufficient number of measurements are made between a pair of holes the data set can be inverted to yield a map of the seismic velocity variations in the plane between the boreholes. A new iterative tomographic inversion technique (the Conjugate Gradients or CG-method) has been developed as part of the project. The CG-method has been compared to other iterative inversion methods and found to give shorter computing times and better reconstruction of model examples. The relative reduction in computing time obtained with the CG-method is of particular significance when large data sets are considered.

The tomographic method has less resolution compared to reflection methods but it provides better quantitative estimates of the values of the measured properties. The tomographic methodology and inversion techniques can also be applied to radar data, but here analysis can be made of both travel time and amplitude data which give maps of radar velocity and attenuation, respectively.

An important insight gained during the project is the high quality of the data (travel times or amplitudes) required for obtaining tomograms without significant artifacts. Techniques for quality control and error correction have been devised and successfully implemented. If these techniques are properly applied tomograms are obtained which are representative of the geological structures in the rock and which do not contain artifacts generated by data errors or the inversion procedure.

The distances between the boreholes at the Crosshole site is at most 200 m. Application of both radar and seismic tomography at these separations have yielded positive results. At the Gideå site borehole seismic signals were registered for borehole separations up to 1000 m.

The crosshole seismic data has also been analyzed with respect to reflections in analogy with the radar. After comparatively complex processing a few reflectors could be identified. Crosshole seismic reflection measurements and analysis is considered to have a potential for describing the geologic structure but further development is required.

At the onset of the Crosshole program no borehole radar existed which could give data on geological structures at appreciable distances from the borehole in crystalline rock. During the course of the project the borehole radar has been developed from essentially a set of good ideas into a practically applicable site investigation tool both with respect to performance of measurement and interpretation of data.

The seismic method has also been developed into a practical site investigation tool both with respect to analysis of data and field procedures.

The comparison of the geophysical results with the hydraulic data from the Crosshole site shows that the features identified are of hydrological significance. Hence the data obtained with the geophysical methods are relevant to the nuclide transport problem.

The access to tools like the radar and seismic methods opens new prospects for the investigation of groundwater flow and nuclide transport through fractured crystalline rock. An important aspect is the possibility to obtain high resolution data on the structure and extent of fracture zones. This could improve the understanding of processes like faulting, lateral variations in the properties of fracture zone, and channeling of groundwater flow within fractures or fracture zones. Data of this type will have bearing on how nuclide transport models are constructed and the reliability of the data that are used as inputs into the models.

3.1.3 Geophysical Model of the Crosshole Site

The bulk of the experimental activities made within the Crosshole program have been performed at a specially prepared site in the Stripa Mine. The site is situated at the end of a drift at the 360 m level (Figure 3-1). Six boreholes have been drilled from the end of the drift in a fanlike fashion. The boreholes outline a tilted pyramid with a height and a base of about 200 m where all boreholes start from the top of the pyramid.

The data from the investigations performed at the Crosshole Site are of three basic types:

– direct observations of geology and measurements of physical properties along the boreholes,

– remotely-sensed measurements of the physical properties of the rock in the space between the boreholes (obtained from radar and seismic measurements),

– measurements of the hydraulic properties of the rock immediately surrounding the boreholes based on assumptions concerning flow geometry.

It should be noted that the hydraulic measurements provide only limited information on the geometry of the water flow paths. In fact, the derivation of hydraulic properties (such as hydraulic conductivity and specific storage) from the field measurements is dependent on knowledge of the flow geometry. Considering the need of the hydraulics for geometrical information, it was considered relevant to construct a geometrical model based essentially on the radar and seismic measurements. The model describes the extent of regions with anomalous physical properties and the magnitude of these properties. In the construction of the model the radar and the seismic data have also been correlated with data of similar type obtained from the single-hole investigations.

The features observed in the radar and seismic data are to a first approximation related to the fracturing of the rock. For example, increases in water content associated with fracturing will cause a localised change in the dielectric constant and electrical conductivity. These changes in electrical properties are then the features observed by the radar. Fractures also cause a decrease in the mechanical stiffness and strength of the rock which, in turn, decreases P and S-wave velocities. These decreases are then observed by the seismic method.

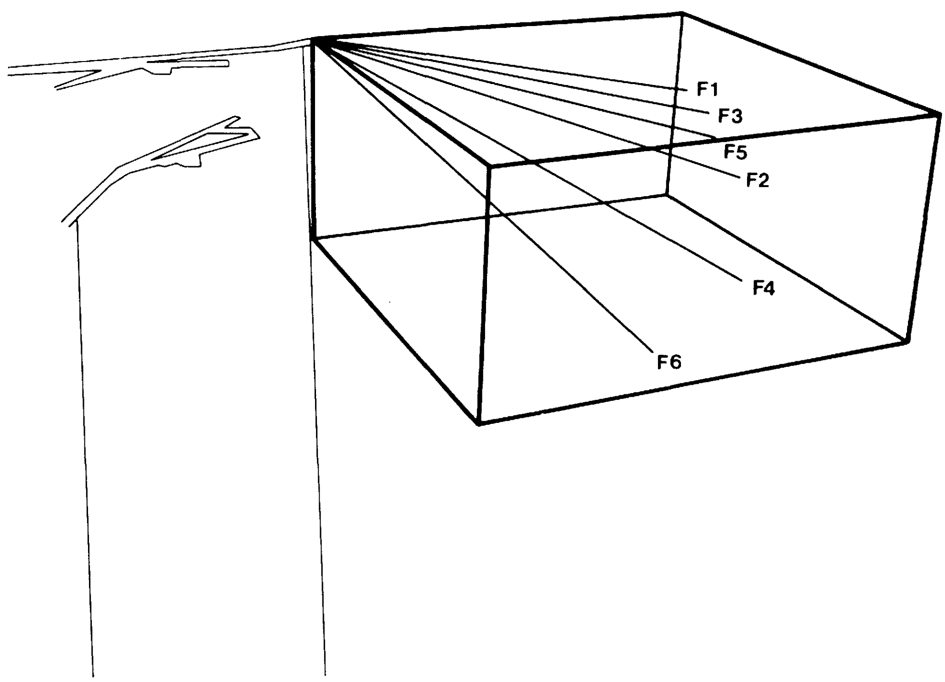

Figure 3-1. Perspective view of the boreholes at the Crosshole site.

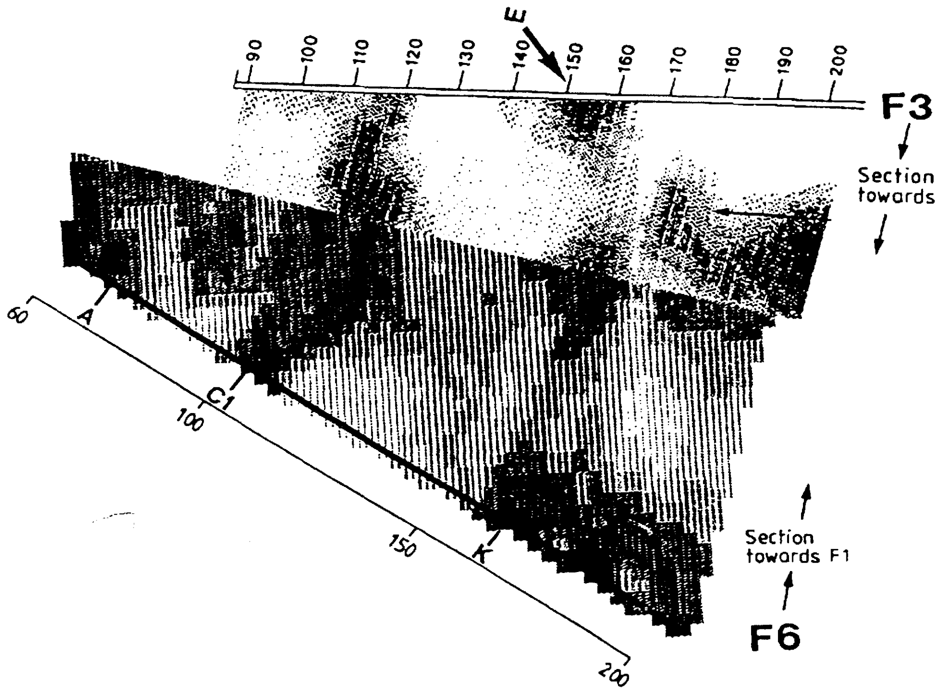

Figure 3-2. Tomograms obtained from inversion of radar amplitudes (F6 – F1 section) and seismic travel times (F3 – F4 section). The intersection line common to both sections occurs approximately in the middle of both sections. The darker colour indicates properties which are indicative of increased fracturing of the rock, i.e. reduced radar and seismic velocities and increased radar attenuation.

However, the radar and seismic methods yield continuously varying fields of electrical and mechanical properties. These are interpreted in the basic geometrical model as two types of rock: heavily fractured and averagely fractured. Hence the geometrical model is a binary one in which regions of heavy fracturing are designated as fracture zones emplaced within background rock. The division between fracture zones and background rock is based on combining the regions of geophysical anomaly seen in tomograms with the occurrence of fractures observed by radar reflection.

The agreement between radar and seismic results is extraordinary and gives confidence that the geophysical anomalies depicted by the tomographic interpretation of crosshole data are real and correctly positioned in space. For example, agreement between radar and seismic tomograms is found where the same section has been measured by both methods and in places where measured sections intersect, i.e. the anomalous features occur at the same locations and have similar form. Intersections between measured sections occur both along boreholes and along lines in the region between boreholes. An example of the agreement between both method and section is the intersection between "F1 – F6 (radar)" and "F3 – F4 (seismics)" shown in Figure 3-2. The line of intersection actually occurs approximately in the centre of the investigated region.

From the tomograms we can see that the darker parts, which represent increased fracturing, form approximately planar regions or zones. However, it is also evident that the geometry of these zones is irregular and that the magnitude of the geophysical anomaly varies within them.

Reflection measurements give information of another type. Reflections are caused by changes in properties and are not very sensitive to the absolute value of these properties. It is apparent from radar reflection results that zones of anomalous geophysical properties are essentially linear features. Some variations in reflectivity and deviations from a straight line can be observed.

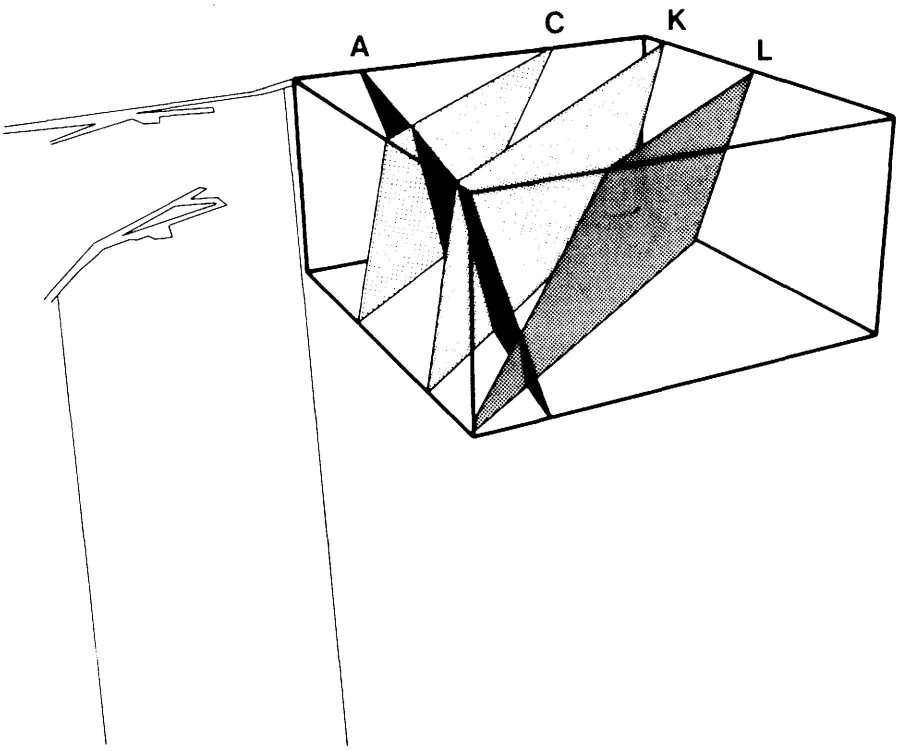

Figure 3-3. Perspective view of the zones included in the Basic Model.

In general, there is good agreement between reflection and tomography data with respect to the location of the major zones. However, because the reflection measurements are more sensitive to changes in electrical properties than the transmission measurements, more zones are seen by reflection than transmission (i.e. tomography).

Two models of the Crosshole Site have been devised. They are termed the "Basic Model" and the "Extended Model". The basic difference between the two is that the Extended Model contains all the features of the Basic Model plus some additional (fracture) zones

The Basic Model contains the most significant zones which have been identified as large anomalies in both the radar and the seismic investigations. These zones have also given significant responses in the single-hole investigations. The existence and location of these zones is considered to be well established and therefore the Basic Model should be highly reliable.

The Basic Model includes zones A, C, K, and L which are observed as prominent features by all geophysical methods. The layout of these zones is depicted in Figure 3-3. from which it is evident that they form two sets characterized by their orientation. The zones C, K, and L are essentially parallel, the strike is NE and the dip is steep towards NW. Zone A has a different orientation. The strike of A is NNE and the dip is steep towards SW. The zones of the Extended model have an orientation similar to zone A.

The Extended Model contains, in addition to the zones included in the Basic model, two other types of zones. The first type of extra zones was identified by only one of the geophysical methods. This results from the differing coverage of the region by the different techniques and includes zones outside the pyramid of boreholes inferred from radar reflection data. The second type is zones which produce smaller anomalies compared to the zones contained in the Basic Model.

The success of the radar and seismic methods is best demonstrated by the concordant description these methods have given of the Crosshole Site. These methods have identified regions in this rock volume of decreased velocity and increased attenuation, properties which both are indicative of increased fracturing. The descriptions agree in many essential aspects; the radar and seismic anomalies appear in the same locations, the anomalies obtained from intersecting planes cut at the same location, and the intersection of the features with the boreholes agree with geological and other geophysical observations. The consistency of the description of the Crosshole site obtained by these methods and the agreement with other results is in a sense a proof of that the methods give a real and relevant description of the rock mass and that the anomalies are not some artifact generated by the method itself or data errors.

3.1.4 Hydraulic Methods

The hydraulic investigations within the Crosshole project have yielded substantial progress in assessing the hydrogeology of fractured granitic rocks. This has resulted from improvements concerning three aspects of hydraulic testing. Firstly the approach to testing has been improved by planning based on reliable geometric information about the whole region to be tested. Secondly the instrumentation used in the testing was computer based resulting in better adherence to interpretation assumptions and improved control over test conditions. Thirdly the testing has demonstrated the application of an improved and feasible interpretation concept which is more appropriate to fractured rocks than previous concepts derived from sedimentary rocks.

As the results of the geophysical measurements were combined with the initial single borehole hydraulic measurements, it became clear that testing effort needed to be focussed on the zones of greatest potential flow. The crosshole testing therefore concentrated on measuring the distribution of hydraulic properties within the extensive fractured zones. Additionally a testing approach using sinusoidally varying pressure and flow rate was adopted to minimise times waiting for the tested zones to regain their pretesting head. This approach for causing a minimum long-term head disturbance during testing was applied throughout the Crosshole programme (i.e. in both single and crosshole testing). It was seen to be effective in reducing waiting times and improving background conditions. The sinusoidal approach to crosshole testing was also seen to be useful in the mine environment since a signal of known frequency is easily observed even against rapidly fluctuating background.

The sinusoidal hydraulic signal was generated by a specially designed and constructed set of computer controlled equipment.

The equipment had several features which were very useful in the mine environment. Firstly, it was possible to generate a precisely controlled signal which conformed closely to the assumptions involved in the analysis of the data. Secondly, the position of the signal was precisely known and the second set of pumps to control the head in the rest of the borehole was extremely effective. In combination with the sinusoidal technique, it was possible, by examining whether there was any sinusoidal variation in the pumping to the rest-of-borehole zone, to evaluate the effective leakage around the packers. Another advantage of the computer control system was the ability to measure to great accuracy using the progressive differential pressure approach. This approach would have been impossible by hand and would have given rise to mistakes which would have damaged some of the components.

In summary, the use of micro-computer to control as well as record tests yielded benefits in improving the quality of the data gathered. The total system which included a novel device to seal the ends of the boreholes resulted in a larger data set being gathered in a limited period.

The form of crosshole hydraulic testing used in the project; that of sinusoidal testing, is sensitive to the geometry of the flow system being tested. When this is poorly known and complex then it is inevitable that only a small number of tests are analyzable. In order to increase the number of well-interpreted tests a new interpretation system based on fractional dimensions has been devised. This analysis uses data from crosshole sinusoidal tests as input to a variable geometry model and derives the apparent "dimension" of the tested flow system in addition to the more usual hydrogeological parameters. Essentially the analysis assumes that there is a continuous spectrum of geometry in between the well-known forms such as 2-D (radial flow in a plane) and 3-D (spherical flow within a porous medium). This is a versatile analysis well-suited to the sort of flow geometries likely to be found in fractured crystalline rocks. It was found that responses were frequency dependent but detailed interpretation of this phenomenon is not yet possible.

The hydrogeology of channelled fractured rocks is broadly understood but relatively poorly investigated in the field. The problem arises from the scale of possible tests. At small scales, such as single borehole hydraulic tests, the flow system can be equated to relatively simple geometries. At the largest scale the rock should behave as an equivalent porous medium. At intermediate scales, such as crosshole testing, the "sparse network" problem arises where test interpretations are particularly difficult.

The hydraulic testing in the Crosshole project has shown some of the possibilities in this field of work. The combination of geophysics with hydrogeology is extremely productive in helping to define problems and focus testing.

3.1.5 Comparison of the Geophysical Model with Hydraulic Data

The geophysical techniques used on the Crosshole Programme were combined to yield the "agreed-on" Basic model of the Crosshole Site. This model is essentially geometrical and as such contains no geophysical appraisal of the hydraulic properties of the identified zones. The zones are identified on the basis of their "contrast", "extensiveness", and their "persistence". The hydraulics data are of a different form since they infer very little (except in special circumstances) of the nature of a "zone" or a fracture away from the immediate vicinity of the borehole.

However, in order to assess the effectiveness of the geophysical techniques in identifying features which are hydraulically important, these two data sets require to be combined or compared.

The hydraulic data, against which the geophysical model is being compared, are of two forms: single borehole and crosshole. The "Basic Model" contains the four zones A, C, K, and L which, with their geophysically determined orientations, should cut the boreholes at 20 points. The "Extended Model" which adds Zones E, F, G, and Unit 1 to the four of the Basic Model should amount to 33 intersections. The thickness of the zones at these intersections is variable depending on the technique used to make the observation. However, it does not exceed 15 m and is seldom greater than 5 m.

Three types of hydraulic anomalies have been defined based on the single hole hydraulic data set; transmissivity, head, and flow.

The most basic data set against which to compare the geometrical model is that of <u>transmissivity</u> (i.e. hydraulic conductivity times zone length). The comparison is achieved by plotting the position of transmissivity "anomalies" and the position of zones from the models. The magnitude of <u>head</u> anomalies is rather more difficult to extract from the testing data than the values of hydraulic conductivity. The head anomalies are defined as the head difference between a calculated head (assuming steady state and porous media flow towards the old drift) and the measured heads for all zones in the boreholes.

A third form of anomaly has been constructed from the single borehole data by multiplying together the previous two. This has the form of transmissivity times head difference which is equivalent to <u>flow</u>. Anomalies defined in this form are measures of the amount of water which would flow into or out of the borehole at a particular location.

The amount of overlap between the various sets of data are shown in Figure 3-4. This shows that the "Flow" anomalies are a slightly closer subset of the geophysical features than any other. The least effective is the head data, but against that the head data are probably the data set which is most poorly measured.

It is apparent that there is a correlation between features identified by single borehole hydraulics and single and crosshole geophysics. It is also apparent that whichever way the single borehole hydraulic data are treated, they yield a naturally smaller group of features than the geophysical data.

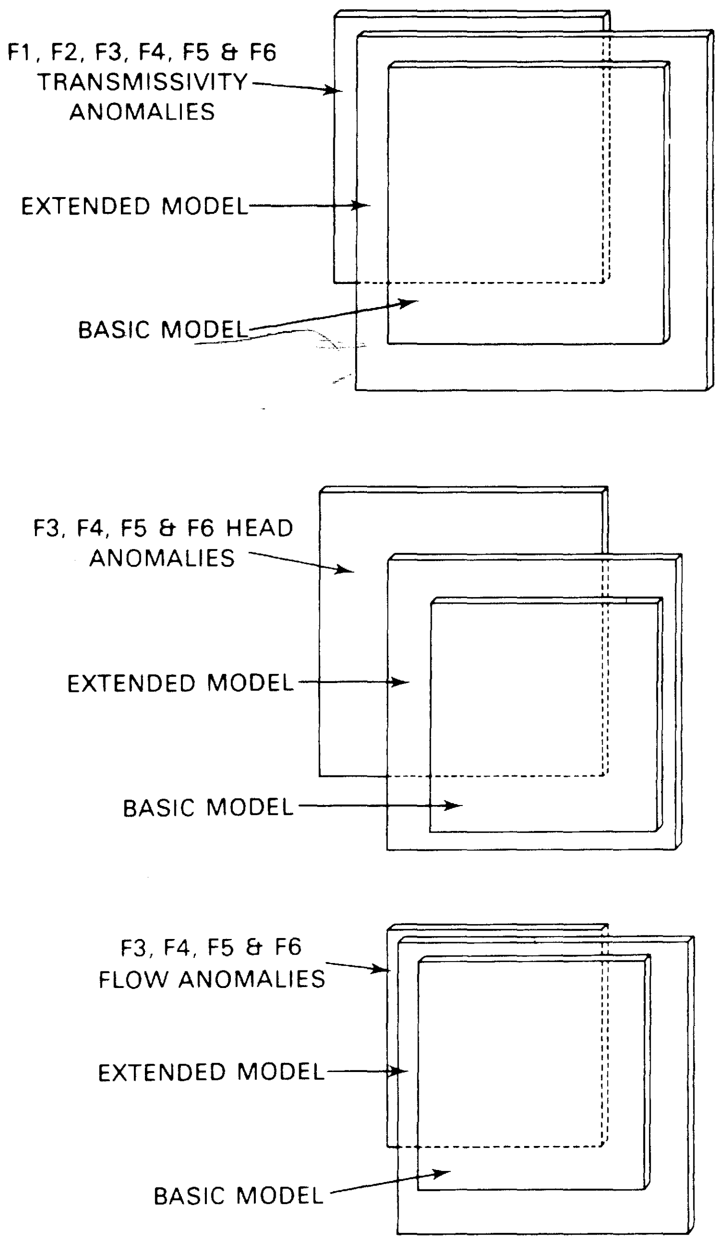

Figure 3-4. The relationship between sets of hydraulic anomalies and the Basic and Extended Models.

3.1.6 Groundwater Flow

The aim of the Crosshole project was to characterize the rock and fractures of the Crosshole site in order to predict the flow of groundwater in fractured granite. A number of different techniques were used to examine the flow of groundwater which resulted in observations at different scales.

At the largest scale (the scale of the whole site), the presence of the "old drift" caused a known head disturbance which was observable at distances up to several hundred metres. The highly variable patterns of head distribution seen in the six boreholes showed that a few "special features" (identified broadly as fracture zones) determined the flow of groundwater within the whole site. Moreover, the fractured granite at Stripa cannot be considered as an anisotropic medium with continuous directional properties.

A series of detailed crosshole sinusoidal tests were carried out to examine the hydrogeological character of two of these fracture zones. These tests showed that, even within the fracture zones, flow was apparently localized to a system of interconnecting channels. The nature of these networks of channels is complex and they differ from zone to zone. The flow testing determined a dimension for these networks which showed that Zone C seemed to have a sparser network of channels and interconnections than Zone A. The testing also indicated that where fracture zones bifurcated they tended towards lower hydraulic conductivity. The hydraulic conductivity derived from single borehole tests within these zones was in the region of $5\ 10^{-8}$ m/s on average.

The crosshole geophysics indicated that the fracture zones consisted of "patches" of more porous rock which were roughly aligned. The patches generally had a major dimension several times larger than the minor dimension. Although it was possible, where crosshole tomograms crossed, to observe these fracture zones in more than one plane, it was not possible to observe the nature of interconnection of patches. Radar reflection measurements tended to over-emphasize the planar nature of fracture zones.

In between the fracture zones which dominate the large scale flow of groundwater, the rock is regularly fractured and some flow occurs within these fractures. This rock was only investigated using single borehole hydraulic tests but again the tests often indicated flow within channels. The testing was not sufficiently detailed to yield the frequency of "active" fractures of channels but it is certainly less than the number of fractures observed by core logging. Analysis of the tests indicated a hydraulic conductivity for this "averagely fractured rock" of about $2\ 10^{-10}$ m/s. This can be compared to unfractured rock which appears to have a hydraulic conductivity around 10^{-11} m/s. However, this value for matrix rock is probably higher that the value which would be measured in the laboratory because it is essentially the material immediately adjacent to the fractures. This may be slightly altered granite rather than the intact rock measured in laboratory experiments.

Overall, the testing showed the need to have a clear idea of the geometry of a potential flow feature before testing. This was because important regions of flow were sparse and spatially comprehensive testing is not possible within conceivable time scales. Additionally the concept of geometry used to interpret the flow test severely influences the values of hydraulic conductivity derived from the results. The hydraulic testing carried out within the programme would have been impossible to organize or interpret without the information provided by the geophysical techniques.

One conclusion that can be made from the combined analysis of the geophysical and the hydraulic data set is that groundwater flow is concentrated within a few major features which have been identified by the geophysical methods. The main features are considered to be broadly planar, containing patches of high and low hydraulic conductivity. The fracture zones are likely to be channelled, where the flow paths constitute a branching interconnecting network.

3.1.7 Implications for Site Investigations

The Crosshole project has demonstrated that there is an optimum structure in a programme of site investigation. This structure needs to ensure that each technique not only expands on information gained earlier but also produces information which is usable later on. The questions of scale and resolution are important to this structure.

In site investigations for radioactive waste, the data will inevitably be used as input to a three dimensional predictive model. The site investigation therefore requires data on the geometry of the site and the distribution of properties within it. Either in the precise region of the repository or wherever the model is to be validated, the model must be capable of reliable and detailed predictions. Hence there must be a structure of increasingly detailed investigations in both time and space.

The first aim of the site investigation programme must be to define the geometry of the major features. Experience from this project shows that the distribution of the major features is identified best by a combination of single borehole reflection radar and tomographic inversion of crosshole radar and/or seismic data. Once these features are identified the second aim can be approached: that is to describe the distribution of important properties such as hydraulic conductivity. This is best achieved by crosshole hydraulic testing even though it is extremely time consuming. In order to solve this problem of time and cost it is necessary to focus the crosshole hydraulic testing on the major features by testing within them. The scales of all these crosshole techniques are relatively large whilst resolution is comparatively coarse. This is most appropriate when the site investigation is at a general level.

The detail of the site investigation can be increased considerably by using the data from high frequency single borehole radar in reflection mode. However, the ability to correlate the smaller radar features with hydraulic parameters is currently not well developed. In general the single borehole radar reflection method indicates more features than are picked out by single borehole hydraulics. The correlation may be improved in the future.

The Crosshole Project has shown that it is possible to characterize fractured crystalline rock with a reliability and realism not attained before. The same approach should be adopted in future site investigations for radioactive waste disposal.

3.2 THREE-DIMENSIONAL MIGRATION EXPERIMENT

3.2.1 General

The general objectives of the experiment are to:

- study longitudinal and transverse dispersion in fissured rock,
- determine flow porosity,
- study channelling,
- obtain data for model verification and/or modification,
- develop techniques for large scale tracer experiments in low permeability fissured rock.

3.2.2 Experimental Design

In the Stripa experimental mine a drift was excavated at the 360 m level below the ground in order to study water flow and tracer migration in low permeability fractured granite. The broader aim is to understand and quantify transport processes relevant to the safety of a final repository for high level radioactive waste.

The drift, which is located in water saturated rock, has a natural inflow of water. The water flowrate to the totally 100 m long drift was monitored by collecting the water in about 375 plastic sheets which were glued onto the ceiling and upper part of the walls. More than 700 m^2 of the drift was covered. In addition the water inflow to the lower part of the drift was measured by a ventilation test. The 125 m long access tunnel, which was excavated in order to ensure that the drift was far away from other tunnels and galleries in the old mine, was also used for a ventilation experiment. Hydraulic heads were measured in three vertical 70 m long holes extending upwards from the drift. Water flows were monitored for more than 2 years.

From the test site which has a total length of 100 m, three vertical holes (length 70 m) were drilled. Within these three holes, 9 different injection zones (each 2.5 m in length) were located at distances varying between 10 and 56 m from the drift. The location of the injection zones within the holes were based on the results from inflow measurements over 2 m sections as well as radar measurements. The space between the injection zones were sealed off with compacted bentonite.

The tracers were continuously injected during 20 months using a small over-pressure. The total injection inflow rates were less than 10% of the total water inflow rate into the upper part of the test site.

Before injection, all 11 tracers were tested in the laboratory and were found to be stable with time and to be "non-sorbing" on crushed granite as well as on the materials used in the equipment. Of these 11 tracers, all conservative, 7 were dyes, 3 were salts and the last one was a high molecular weight tracer. The 7 dyes were selected based on tests of 100 different dyes.

From the most water conductive sampling areas (65 areas) water samples were taken every 16 hour. Samples were also taken from another 80 places, such as sampling areas with low water flow rates, wet spots on the floor, adjacent boreholes and drifts. The time intervals between samples from these places were 1–5 weeks, depending on the water flow rates. The water sampling continued 6 months after the end of injection.

3.2.3 Results

The water flowrates varied very much between the different sheets. One sheet carried 10% of the total water flow to all the sheets. 50% of the water came to about 10 of the sheets, 90% of the water came to 42 of the sheets or about 10% of the covered area.

The average hydraulic conductivity of the covered area was found to be between $0.4 \cdot 10^{-11} - 0.8 \cdot 10^{-11}$ m/s. The floor and lower sides have a conductivity of $2 \cdot 10^{-11} - 4 \cdot 10^{-11}$ m/s and the average of the access drift was $0.5 \cdot 10^{-11} - 1 \cdot 10^{-11}$ m/s.

The variations along the experimental drift were so large that it is doubtful if the 100 m long drift was long enough to make up a "Representative Elementary Volume" (REV) of an equivalent porous medium.

Tracers were analyzed for in all sheets carrying water and in some locations in the floor of the drift where water was seeping out. Many of the tracers were strongly colored dyes and were looked for in other drifts and galleries as well as in waters sampled in other places in the mine. The tracer concentration curves for 6 of the tracers which arrived in measurable concentrations, in all 167 curves, were analyzed by fitting them to several different models which describe tracer transport. 25 of the curves representing most of tracer flowrate were analyzed in more detail. The models were the Advection-Dispersion model, the Advection-Channeling model and two models based on the previous two, to which is added the further mechanism of molecular diffusion of the tracers into and out of stagnant pools of water. The fitting of the models to the experimental concentration curves gave values of the mean travel time of water from the different injection points and also information on dispersion. Matrix diffusivities for the tracers were measured in the laboratory and the second set of models were used in an attempt to determine values of the frequency of water conducting fractures and the average amount of fracture surface in the rock which was in contact with the mobile water.

The travel times were found to vary between 2000 and 7000 hours as averages for the tracers, but considerably shorter as well as longer times were found in some of the sheets.

The flow porosity determined from these data was $15.5 \cdot 10^{-5}$ for the tracer injected nearest to the drift. The porosity decreased with increasing distance and was $2 \cdot 10^{-5} - 3 \cdot 10^{-5}$ at the farthest injection points. The higher porosity near the drift was interpreted to be caused by the change of rock stresses induced by the presence of the drift.

The dispersivity was found to be very high for all except one tracer. Peclet values of less than 4 were obtained for two of the tracers. For two of the tracers values around 5 were typical and for one of the tracers values around 30 were found. The low and very low values are deemed to be caused by other mechanisms than what is usually included in the term hydrodynamic dispersion. The main cause seems to be channeling, i.e. the transport of the tracer in a few channels with different transport properties. The presence of "channels" or some preferential pathways was also noted by the presence of tritium in some of the holes. The tritium must have been carried from surface waters in a time period less than 30 years.

The recovery of the tracers varied between 2.8% and 65% for 5 of the tracers. One of the tracers had a recovery of 0.002%, four were not found at all, and one was recovered in a considerable but unknown quantity. The tracers which were not found were, as a rule, injected at the farthest distances.

The recovery data were used to analyze the possibility of matrix diffusion and diffusion into stagnant pools of water as a cause for the loss of tracer. The analyses show that both mechanisms are probably active and will cause the loss of tracer to some extent. It cannot be ruled out, however, that there are also other causes for the loss of tracer. One tracer which was injected 18 m above the drift was found to have travelled more than 150 m to the newly excavated gallery in a considerable quantity.

It cannot be ruled out that also some of the loss of the other tracers may be due to transport to some other location, although with the exception of one tracer no traces of the tracers have been found in the water samples taken in many other parts of the mine.

The conventional models used in the evaluation of this experiment cannot be used without modification to accurately and in detail describe the movement of water of tracers in the Stripa rock. The variability of rock properties is very large and results will be strongly influenced by local variations of the properties.

The variability in the data obtained in this investigation may, however, be useful in stochastic models which then may also indicate not only expected average properties but also the expected variability in the properties.

3.3 ECONOMY

The total cost of the Stripa Project Phase 2 as of December 31, 1987 is given in the Table 3-1 below.

Table 3-1. Stripa Project Phase 2 – Summary of costs as per December 31, 1987. All figures in SEK.

	Total program			
Program	**Original budget incl 10% annual esc.**	**Rev budget 1986 incl 10% annual esc.**	**Accumulated**	**Estimated Remaining**
Project management	3 700 000	6 000 000	4 521 244	1 478 756
Mine operations	14 150 000	12 400 000	12 320 496	79 504
Crosshole techniques	22 400 000	22 800 000	23 123 401	-323 401
3-D tracer experiment	8 350 000	9 250 000	8 848 373	401 627
Sealing test	10 200 000	9 900 000	9 898 523	1 477
Hydrogeological characterization	260 000	900 000	881 968	18 032
Hydrochemistry	1 400 000	3 240 000	2 912 016	327 984
Seismic crosshole	700 000	890 000	859 482	30 518
Total	**61 160 000**	**65 380 000**	**63 365 503**	**2 014 497**

4 PHASE 3

4.1 SITE CHARACTERIZATION AND VALIDATION

4.1.1 Drilling

The new previously unexplored site used for the experiments included in the Site Characterization and Validation Project is located West of the 3D-migration site and Northeast of the BMT-area (Figure 4-1). The drilling of the six boreholes at the new site started in the beginning of September 1986 and was completed in the beginning of December. The drilling could be carried out with out any serious problems.

Three holes are directed towards the North, two towards the West and one borehole is vertical. The near horizontal holes are 150 – 220 m in length while the vertical hole is 50 m long. The exact position of the boreholes in the local mine coordinates and other data is given in Table 4-1. The total length of the holes drilled within Stage I is 960 m. The holes are 76 mm in diameter and fully cored.

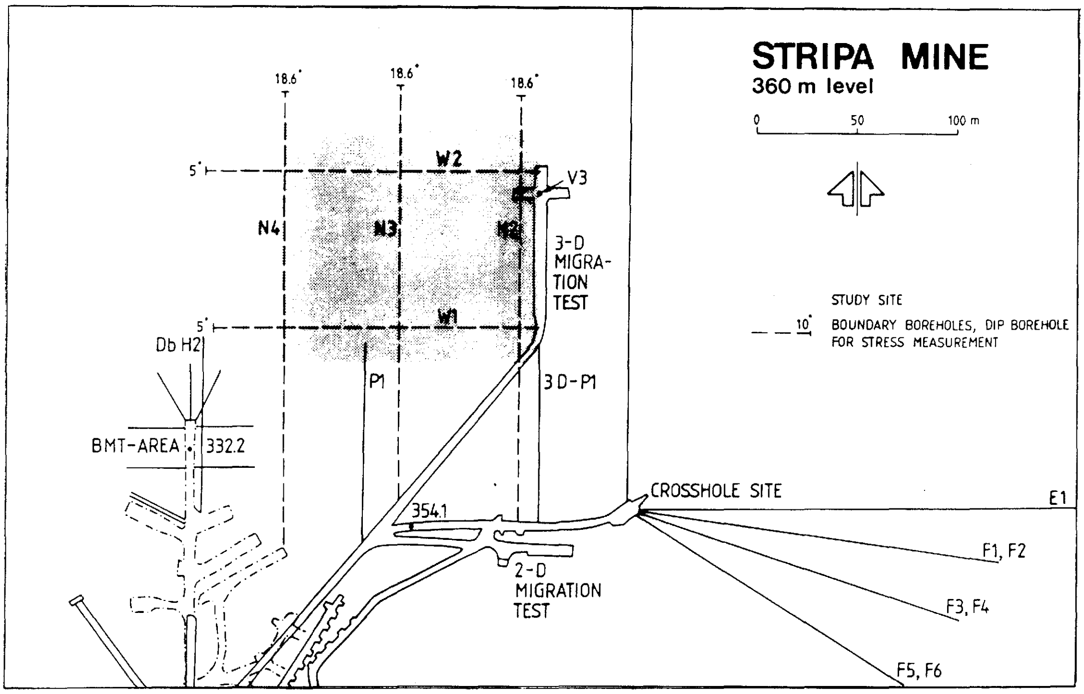

Figure 4-1. Plan view of the Stripa Mine at the 360 m level showing the position of the SCV-site and the Stage I boreholes.

Table 4-1. Position of boreholes W1, W2, N2 – N4, and V3, in the local mine coordinates. Declination from mine north (in degrees), inclination below horizontal plane (in degrees), length (m), together with date for start and completion of drilling.

	W1	W2	N2	N3	N4	V3
Collar position:						
X	440.0	510.0	333.3	347.4	321.1	502.9
Y	1146.8	1147.4	1139.2	1079.1	1023.1	1149.7
Z	356.1	355.3	356.7	356.9	345.0	356.5
Bottom hole position:						
X	441.7	511.4	530.1	527.4	529.0	503.4
Y	1000.3	1000.8	1141.0	1082.6	1025.5	1149.7
Z	368.1	365.9	420.7	414.2	413.7	404.5
Collar deviation:						
Declination	269.94	269.90	359.85	359.97	359.25	
Inclination	4.99	5.02	18.59	18.59	18.80	89.33
Bottom hole deviation:						
Declination	271.39	271.19	0.87	2.20	2.12	
Inclination	4.13	3.32	17.31	17.01	17.47	89.49
Length	147	147	207	189	219	50
Drillstart	861023	861105	861006	860917	860829	861201
Drillstop	861103	861120	861016	861001	860911	861204

4.1.2 Head Monitoring

A system for head monitoring has been set up in the Stripa Mine to follow changes in hydraulic head caused by drilling and experimental activities at the new site. The head has been monitored is 26 measuring points surrounding the Phase 3 site. Measurements have been taken in intervals from one to six hours. Prior to the installation of the automatic Piezomac system manual recording was made in a set of boreholes.

Figure 4-2 displays the head variations in some of the R-boreholes in the BMT-drift during the time of the drilling. The head variations were relatively small when the first four boreholes were drilled but when about half of borehole W2 had been drilled a large reduction in head could be observed in most of the holes where the head was monitored. After the drilling of W2 had been completed the hole was sealed and the heads started to increase. The head variations in borehole N1 during a three month period following the installation of the Piezomac system are shown in Figure 4-3. The rapid drops in recorded head are associated with the opening of borehole W2 in order to perform measurements in it. The head changes caused by opening and closing of W2 are large and can be observed over large distances. The distance between the middle of W2 and the bottom section of N1 and the R-boreholes are both roughly 160 m.

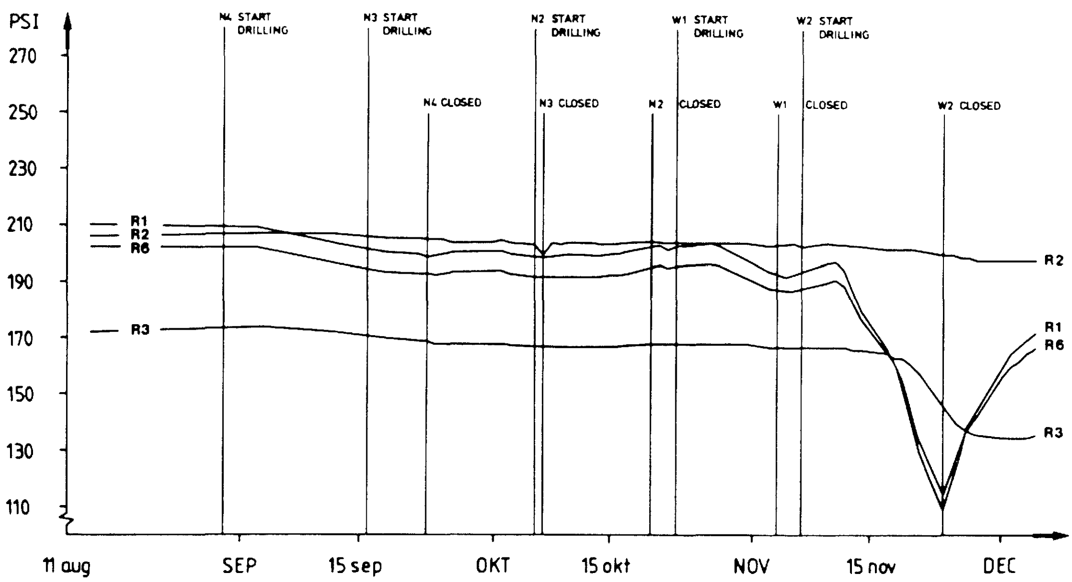

Figure 4-2. Head variations in some of the R-boreholes in the BMT-drift during the time of drilling.

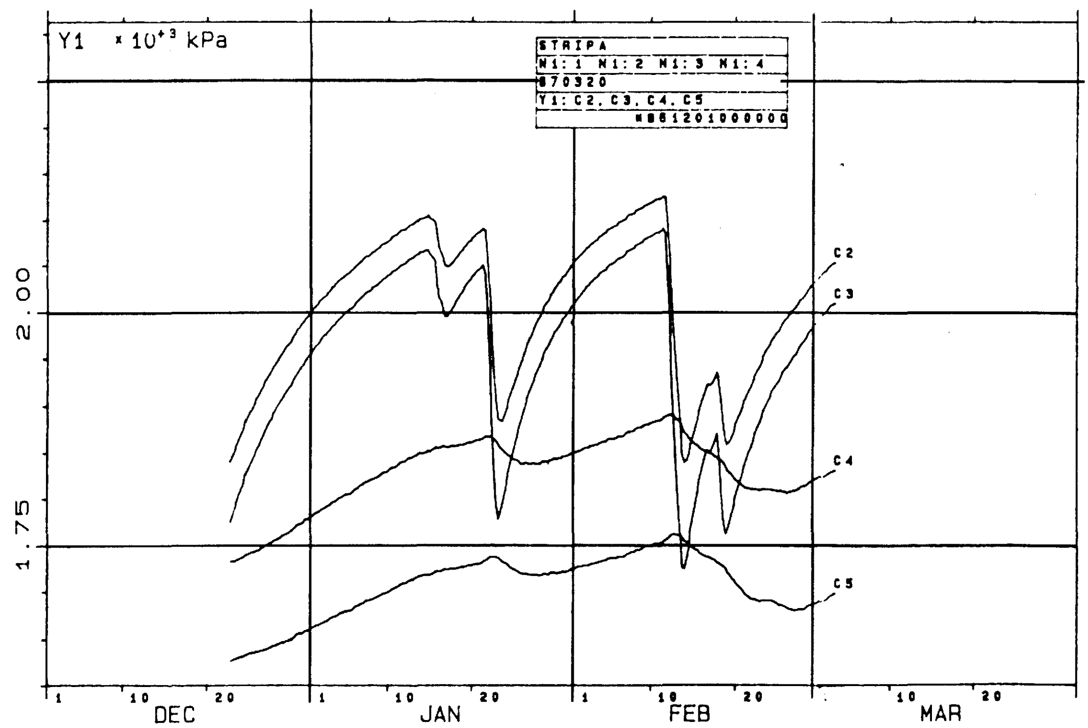

Figure 4-3. Head variations in borehole N1 from December 1986 to March 1987. Borehole sections; C2: 252-300 m, C3: 152-250 m, C4: 120-150 m, C5: 10-118 m.

4.1.3 Single Hole Geophysical Logging

To achieve comprehensive knowledge of the physical conditions in the rock mass in the vicinity of the boreholes the following geophysical borehole methods have been used: borehole deviation, natural gamma ray, neutron – neutron, sonic, single point resistance, normal resistivity, temperature, borehole fluid resistivity (salinity), and televiewer.

The porosity of the bedrock has been calculated using the resistivity measurements. In borehole N4 both a thermal and an epithermal neutron measurement have been performed, showing both methods to be influenced mostly by the water content in the fractures. These methods are accordingly very good "water indicators".

The mean value of the physical properties of the rock surrounding the boreholes is given in Table 4-2. In each of the boreholes, major units of deformed and/or fractured rock have been distinguished. These major units exhibit anomalous physical conditions and therefore cause marked responses on several logs.

Table 4-2. Approximate mean physical properties.

Method	W1	W2	N2	N3	N4	V3	Unit
Normal res.	70	50	100	80	80	150	kOhmm
Single Point	40	40	40	30	40	30	kOhm
Porosity	0.8	1.0	0.5	0.4	0.4	0.3	%
Thermal neutr.	5.0	5.0	5.0	5.0	5.0	5.0	kcps
Temperature	11	11	11	11	11	11.5	deg C
Salinity	150	150	280	300	330	170	ppm
Sonic	6.1	6.0	6.0	6.2	6.0	6.0	km/s
Gamma ray	70	–	80	70	70	70	μR/h
(Radon)	140	200	200	–	125	–	μR/h

The following details should be noted when studying Table 4-2;

- Borehole V3 shows the highest Normal resistivity and a corresponding low porosity, thus indicating the least fractured/altered rock.
- Borehole W1 and W2 have a slightly less Normal resistivity compared to boreholes N2, N3, and N4, thus indicating less fractured rock in the latter boreholes. The porosity results supports this interpretation.

A schematic comparison between coated fracture frequency (from the core mapping) and porosity (from the logs) shows that the fracture frequency controls the porosity variation. Furthermore, the matrix porosity can be determined. In W1 and W2 zero fracture frequency thus corresponds to 0.4 – 0.5% porosity, while in N2, N3, and N4 the matrix porosity seems to be in the order of 0.1 – 0.2%.

The specific geophysical character of the deformed units enable correlation of some of the units between the boreholes, assuming the units to be planes. The main direction of the units seem to be N – NNW, and steeply dipping. Furthermore, the zones heading within the direction NW to NE seem to constitute the dominating path for water movement within this part of the Stripa granite. Apart from these zones, the granite is relatively competent, probably exhibiting low hydraulic conductivity.

Pegmatites and concentrations of darker minerals have been recognized.

4.1.4 Borehole Radar

The borehole radar investigation program has comprised single hole reflection measurements with centre frequencies of 22, 45, and 60 MHz. The frequencies 22 and 45 MHz have been used in the boreholes N2, N3, N4, W1, and W2. Reflection measurements with the centre frequency 60 MHz were made in V3 prior to and after the rock stress measurements (hydrofracturing) in that hole. Crosshole tomographic measurements have been made between the boreholes W1–W2, N2–N3, N3–N4, and N2–N4. Crosshole reflection measurements have also been made between the same boreholes. The reflection measurements were made with the transmitter fixed at three positions in each borehole while the receiver was moved in 1 m increments in the other borehole. All crosshole sections were measured with the centre frequencies 22 and 60 MHz, except N2–N4 which was measured only with the lower frequency. The entire measurement program has totalled over 20 000 rays.

The radar range obtained in the single hole reflection measurements was approximately 100 m for the lower frequency (22 MHz) and about 60 m for the centre frequency 45 MHz. In the crosshole measurements transmitter-receiver separations from 60 to 200 m have been used.

An integrated analysis has been performed of the radar results obtained from the three different measurement modes. From the processed radar data geometric information about the location and extent of major features has been extracted. The geometry of the boreholes has forced radar data to be collected in two different planes, i.e. the N2–N3–N4 and the W1–W2 planes. Both planes are semi-horizontal with the W1–W2 plane located above the other plane. The borehole geometry has given a better definition of the major features in the planes of investigation compared to other locations within the site.

The radar model of the site includes three major features (fracture zones) and four minor zones. The location of these features in the N2–N3–N4 and the W1–W2 planes are displayed in Figures 4-4 and 4-5, respectively. The zones RA, RB, and RH are con-

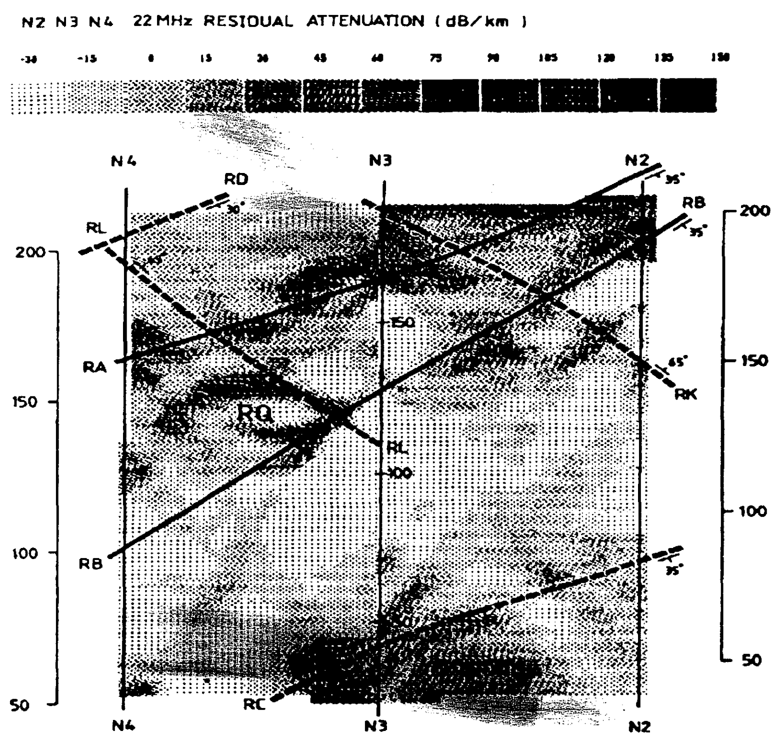

Figure 4-4. Tomographic map of radar attenuation in the borehole section N2–N3–N4. The location of the major and minor features included in the radar model of the SCV site is indicated.

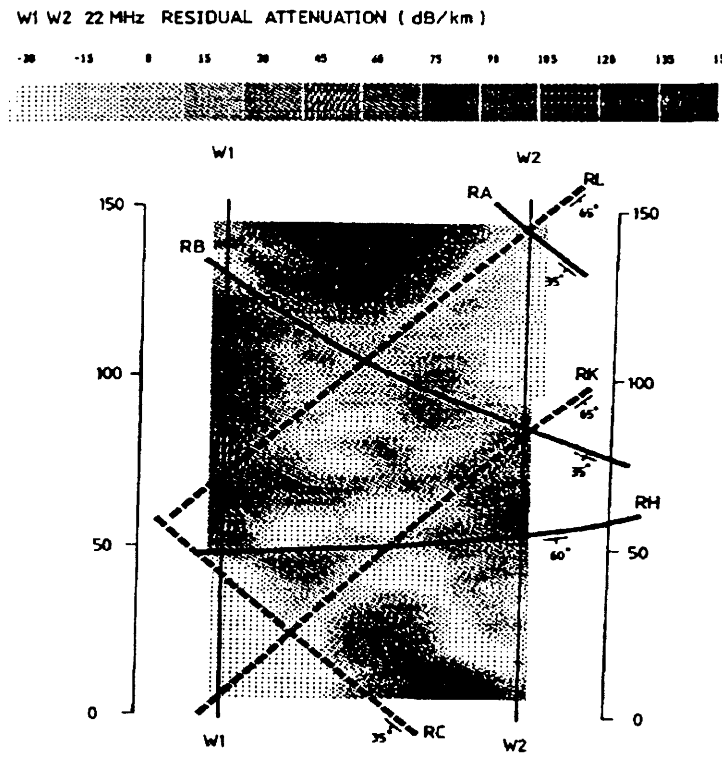

Figure 4-5. Tomographic map of radar attenuation in the borehole section W1 – W2. The location of the major and minor features included in the radar model of the SCV site is indicated.

sidered as major zones while RC, RD, RK, and RL are of smaller magnitude. The zones can also be grouped according to their orientation. The zones with a northeasterly strike (N35 – 40°E) and a dip of approximately 35° to the South are RA, RB, RC, and RD. Zones RK and RL are almost perpendicular to this set and have a strike of N55°W and a dip of 65°N. The zone RH strikes N5°W and dips steeply ($\approx 60°$) to the East.

The zones, as they are seen from the tomograms, consist of a number of patches of increased attenuation and slowness following lines in the planes between the boreholes. Increased slowness and/or attenuation corresponds to increased porosity, fracturing, and/or alteration of the Stripa granite. The results indicate that the zones are not homogeneous but rather that they are highly irregular containing parts of considerably increased fracturing and parts where their contrast to the background rock is quite small. The zones appear to be approximately planar at least at the scale of the site. If the geometry of the zones are studied at a smaller scale the planar nature of the zones might be less obvious. At the smaller scale the patchiness becomes dominating and the zones can appear quite irregular.

One of the most extraordinary features in the attenuation tomograms is the circular feature (RQ) between boreholes N3 and N4. The existence of the feature and its shape must be considered to be real and no artifact produced by errors in the data or the tomographic inversion procedure. The feature appears both in the two attenuation tomograms from the borehole section N3 – N4 and in the borehole section N2 – N4. Even though the tomograms originate from two different data sets the resulting anomaly is located in the same place and has the same shape in both tomograms. This fact can be considered as strong evidence that the location and shape of the feature is correctly represented in the tomograms.

The radar investigations have given a three dimensional description of the structure at the SCV-site. A generalized model of the site has been produced which includes three major zones, four minor zones, and a circular feature. These features are considered to be the most significant at the site. Smaller features than the ones included in the generalized model certainly exist but no additional features comparable to the three major zones are thought to exist. A study of the minor features would require a more detailed analysis of the data.

4.1.5 Crosshole Seismics

Seismic crosshole and reflection measurements have been performed at the Site Characterization and Validation Site (SCV – site). Three sections were measured, one between the boreholes W1 and W2, one between N2 and N3 and one between N3 and N4.

The receiving units used during the experiment were of two types, one developed at FOA and the other by Vibrometric OY. Two types of seismic sources were used, a mechanical hammer and a sledgehammer. The hammer type source, which is developed by Vibrometric OY, was used for borehole to borehole measurements and the sledgehammer for drift to borehole measurements. The data recording was made with a field computer system developed at FOA.

The results from the W1 – W2 section are from two sets of recordings; one with the hammer source in W1 and receivers in W2 and another with the sledgehammer-source in the drift and receivers both in W1 and W2. The last set formed VSP – like sections which were used in the reflection analysis. A total of 960 rays were recorded for this section.

The N2 – N3 and N3 – N4 sections were measured simultaneously by placing the source in N3 and receivers in both N2 and N4. 490 rays were recorded for the N2 – N3 section and 460 for the N3 – N4 section. No measurements from the drift were done for these sections.

The tomographic analysis involves the following steps:

– First arrival time picking.

– Time-offset corrections.

– Anisotropy corrections.

– Data checks (removal of rays with large residual errors) .

– Tomographic inversion.

The analysing routines have been improved during Stage I. A new analysis package, including the steps described above, has been developed which has increased the speed of the analysis work considerably.

The method of analysis of seismic reflections is under development as a separate research within the present phase of the Stripa Project. The application in this stage should be considered as a trial.

The interpretation procedure can be divided in two parts, the filtering in two dimensions and the calculation of the geometry of the reflectors. The first part consists of:

– minimum phase band-pass filtering,

– data adaptive deconvolution,

– Tau-p filtering,

– coherency stack.

The second step of the interpretation procedure attempts the construction of a geometrical model consistent with the position and shape of the reflected events observed in several time-depth profiles. In the present case, the model was the one inferred from the tomographic analysis.

The tomographic analysis reveals a rather complicated structure, in contrast to the results from measurements at the Crosshole site during Phase 2 of the Stripa Project (Pihl et al. 1987, Olsson et al. 1987). The structures at the Crosshole site are more linear than at

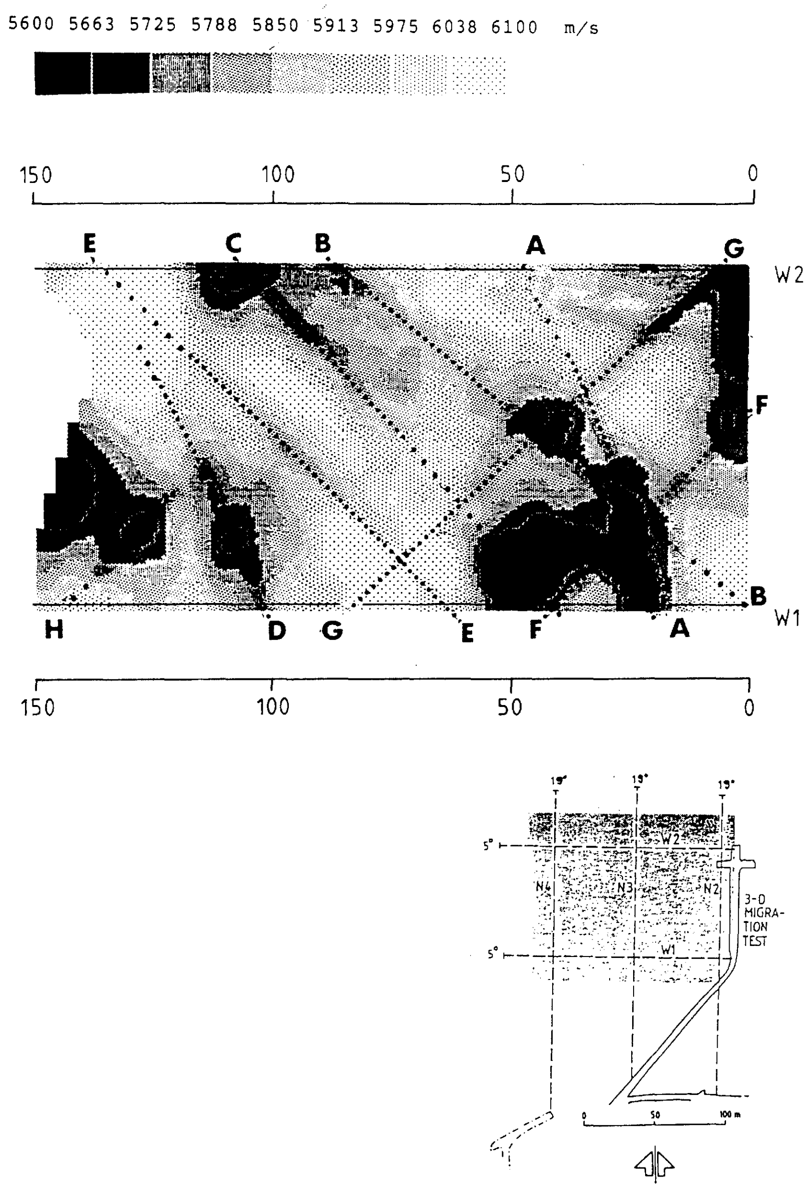

Figure 4-6. Tomographic reconstruction of the sections N2–N3 and N3–N4. The number of iterations was 50 and the damping factor 20.

the SCV-site where they appear more "patchy". The velocity variations are larger at the SCV-site (10% and 2% respectively). The anisotropy, however, is low at both sites; 0.5% in the SCV-site and zero at the crosshole site.

If both sections are viewed at the same time, and also reflections are considered, some ten features can be identified. Figures 4-6 and 4-7 display tomograms over the sections Wl–W2, N2–N3 and N3–N4 calculated in the standard way. The features or fracture zones are marked with letters from A to J. The corresponding reflection profiles from the boreholes Wl and W2 are shown in Figures 4-8–4-10.

Figure 4-11 shows the result of a tomographic analysis of the Wl–W2 section where only borehole to borehole data has been used. The features are less sharp here especially those which run at small angles to the boreholes.

In order to further investigate the nature of the anomalies a tomographic inversion with a smaller damping (half the normal) was performed (Figure 4-12). When lower damping

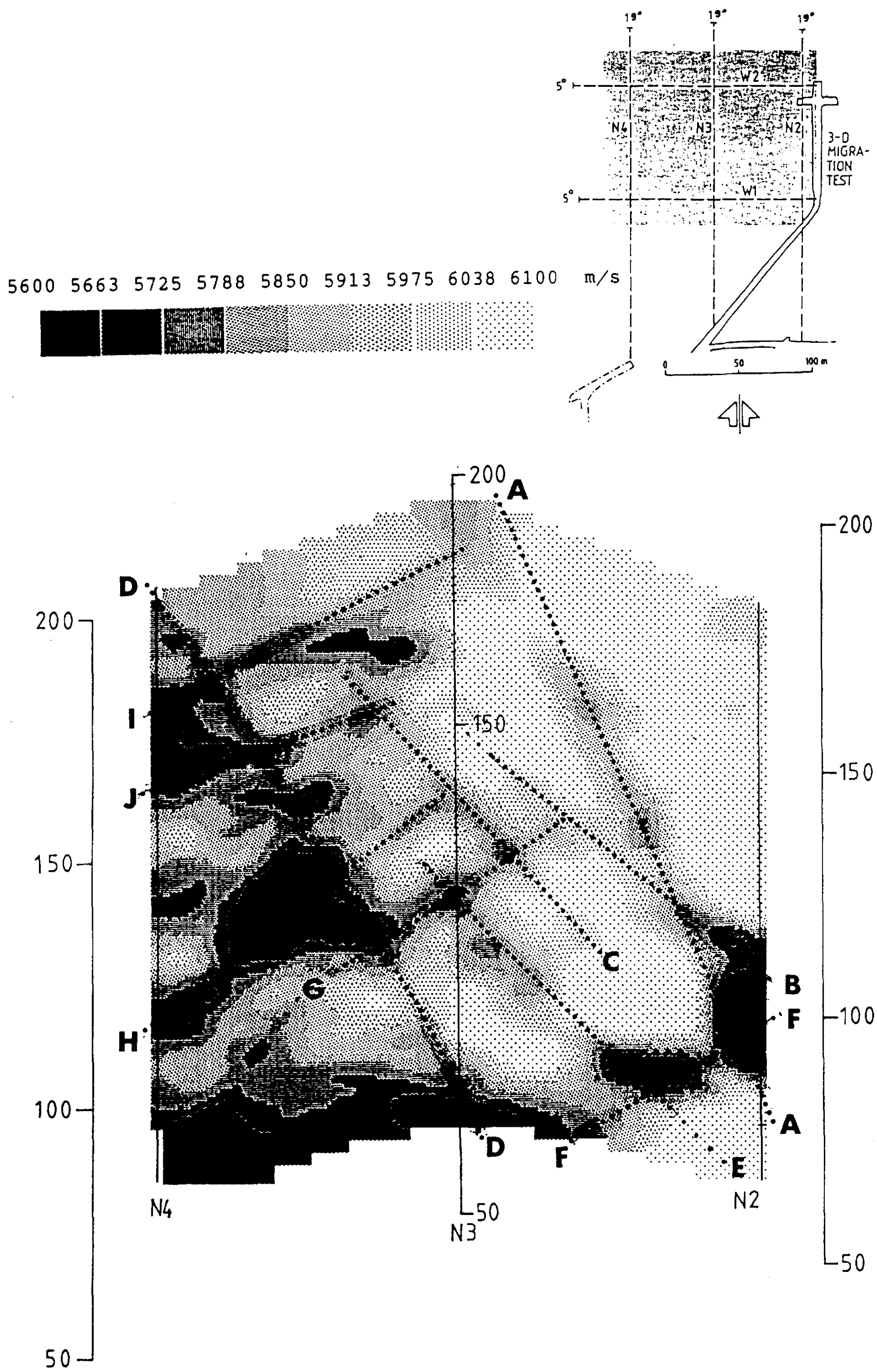

Figure 4-7. Tomographic reconstruction of the section W1 – W2. The number of iterations was 50 and the damping factor 20.

is used the result becomes noisier. However, in some cases the increased sharpness can be useful. The "patchiness" in the features is even more clear in Figure 4-12.

The suggested orientations of the zones fall into two groups. One in a north – easterly (N45 E – N70 E) and one in a north – westerly direction (N25 W – N60 W). These orientations are different from those found at the Crosshole site, which were N225 E and N10 E.

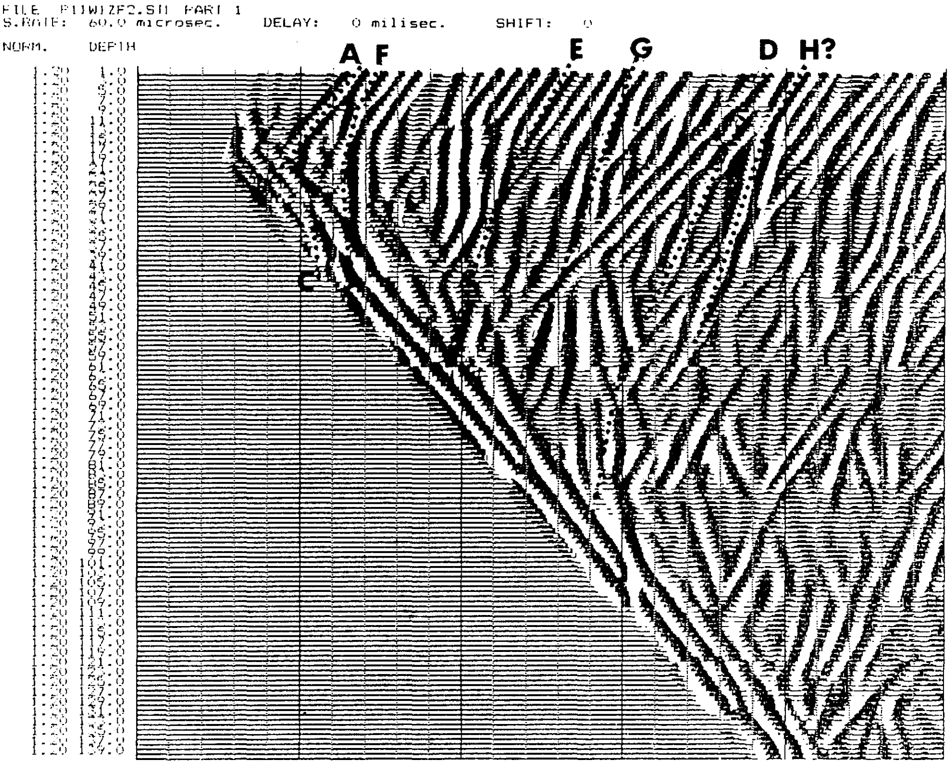

Figure 4-8. Reflection profile (zero offset VSP) from borehole W1. The shotpoint is near the top of the hole.

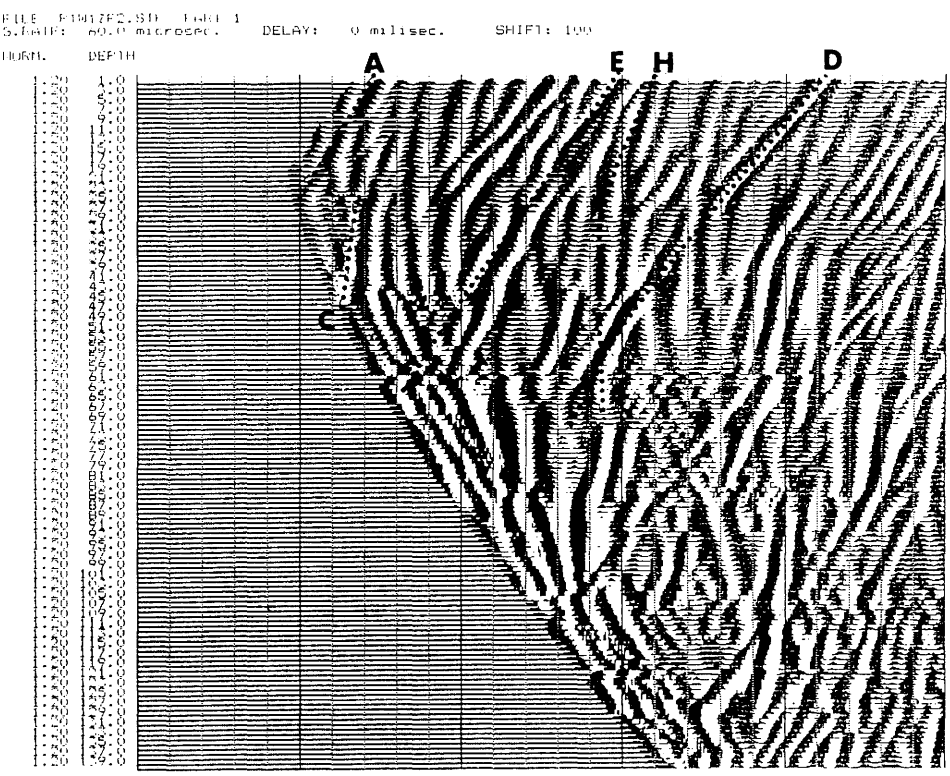

Figure 4-9. Reflection profile (offset VSP) from borehole W1. The shotpoint is 70 m offset from the top of the hole.

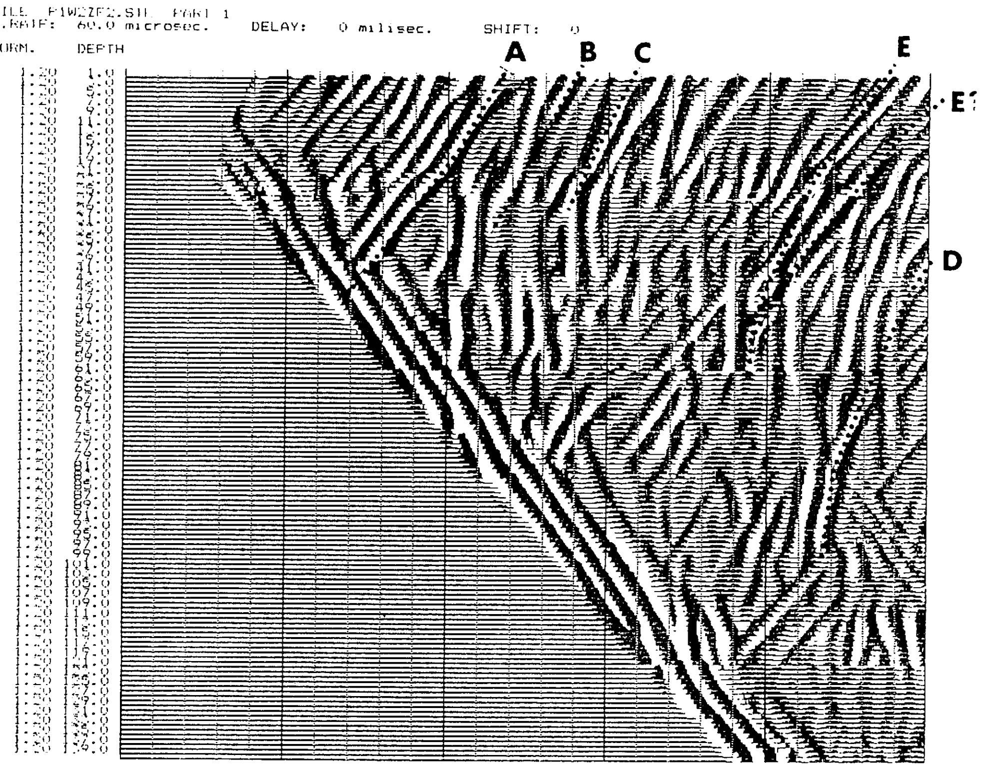

Figure 4-10. Reflection profile (zero offset VSP) from borehole W2. The shotpoint is near the top of the hole.

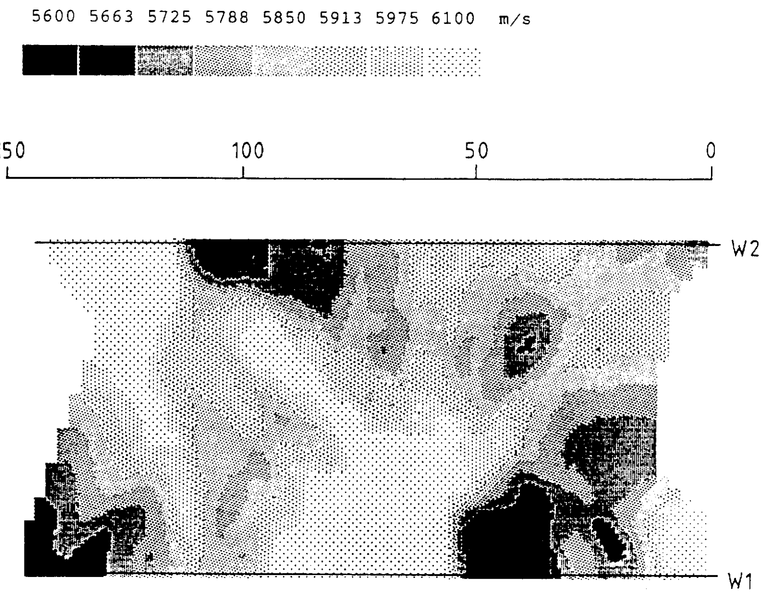

Figure 4-11. Tomographic reconstruction of the section W1—W2 from only borehole to borehole data. The number of iterations was 50 and the damping factor 20.

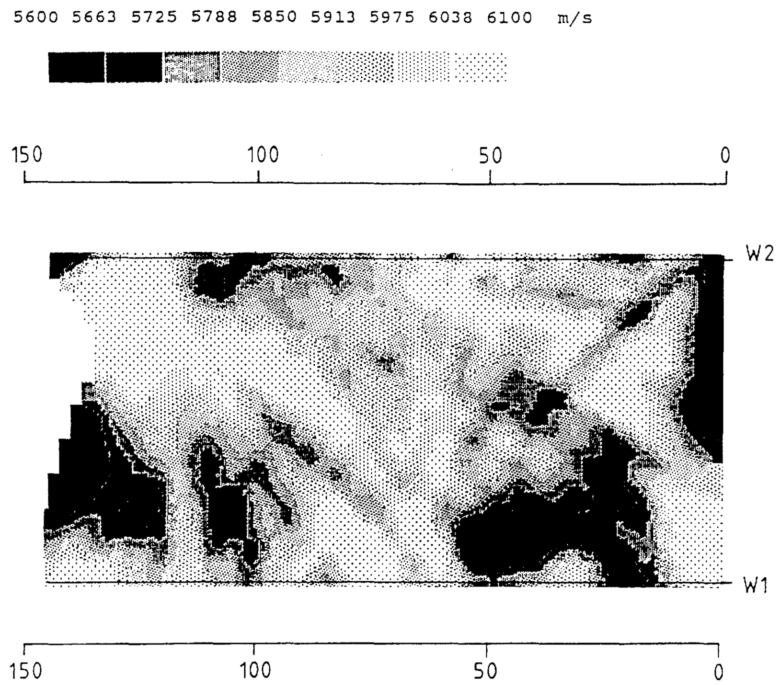

Figure 4-12. Tomographic reconstruction of the section W1 – W2. The number of iterations was 50 and the damping factor 10.

4.1.6 Hydraulic Investigations

Aims and Objectives

The aim of the hydraulic investigations which form part of the Site Characterization and Validation (SCV) Project is to provide data for input to the groundwater flow model of the "virgin site". Since it is envisaged that the eventual model will be some form of deterministic/probabilistic (network) hybrid the hydraulic data must be suitable for both types of application. Additionally another use of the hydraulic data is to gain some corroboration in places (by virture of measured heads) of the rightness of the geophysics based geometric model of the site.

In this first stage of the SCV Project the intention was to gather data for a preliminary modelling of the site. Hence the test programme was of a reconnaissance form and was based on hydraulic tests in single exploratory boreholes.

Background

The novel aspect of the SCV Project is the attempt to apply probabilistic network models to a site characterization. The aspect of probabilism means that at large data set is desirable especially concerning those features which most affect the flow properties of the whole rock mass. In a fractured crystalline rock the fractures are obviously the paths for water flow. In the SCV Project much effort is going into the mapping of fractures and the assignment of those fractures and their characteristics to different fracture sets. Hence the hydraulic programme was geared to measuring the hydraulic properties and heads of the fractures. Thus although this was designed as a reconnaissance programme it was necessary to devise a programme of testing which would measure as many individual fractures as possible. Given the number of fractures in the rock mass and their frequency it is clearly impossible (in a reasonable period) to measure the hydraulic properties of every single fracture. In order to overcome this problem, it was decided to concentrate on the most important fractures. This resulted in the adoption of the approach known as "focussed testing".

Focussed Testing

The idea of "focussed testing" is to concentrate the effort involved in the testing so that the most conductive fractures are measured in most detail. Ideally the most conductive fractures would be measured individually and focussed testing aims to achieve this by having a variable straddle interval. This means that "focussed testing" requires a packer system where the straddle interval can be altered within the borehole. Another requirement of this approach, since the straddle interval needs to be varied according to the value of transmissivity, is that the transmissivity needs to be determined as testing proceeds. This requires field-based interpretation. The solution to the variable spacing packer problem is the "active packer string" (see Figure 4-13).

In order to carry out this approach an "active packer string" has been designed, built and used in the Stripa Mine during 1987. It has been designed and built in collaboration between BGS and SGAB. The system has several features which make it unusual. They are:

1) The string of five packers can be individually inflated.
2) The packer inflation and test implementation is controlled by micro-computer (a number of different tests are possible).
3) Tests can be interpreted in the field as they are being carried out using a second networked micro-computer.

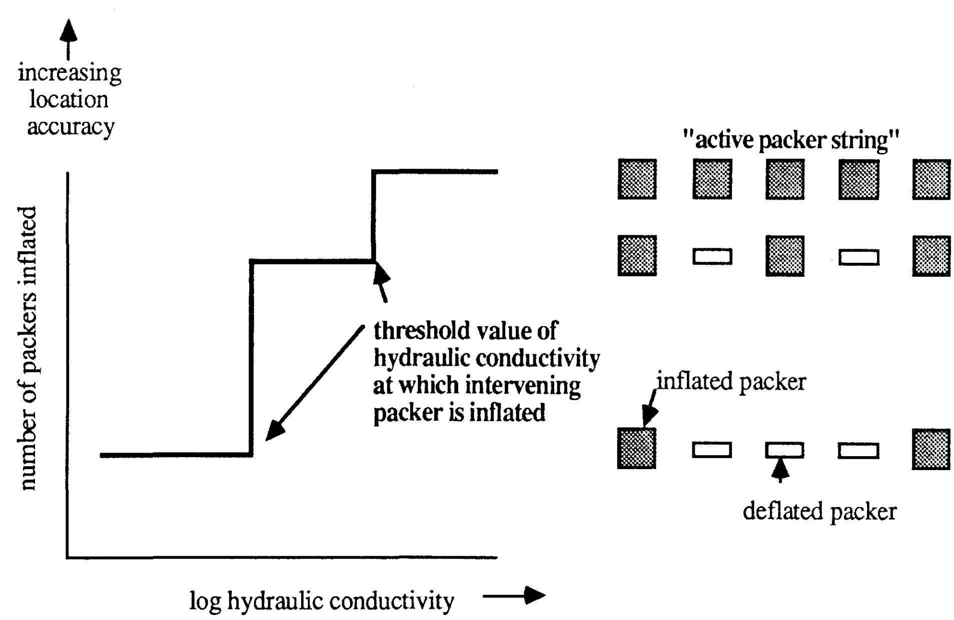

Figure 4-13. The use of the "active packer string" to change the straddle packer length so that highly conductive fractures are most likely to be measured individually.

From the field operators viewpoint a zone is tested first using the coarsest 7 m interval. If the transmissivity exceeds a pre-set value, the intervening packer is inflated and so on. By changing the value at which the intervening packer is inflated the duration of the testing and the number of maximum definition fractures is altered.

During the year, significant effort was involved in developing the test control software to avoid over-pressurizing the test interval. A complementary problem concerning the compliance of the packers was solved by developing a large diameter mandrel with plug-in connections. Since the system was entirely computer controlled there were a large number of solenoid activated valves. Some reliability problems were encountered with long term operation of these valves.

Results

The five boreholes were tested in order N3, N2, N4, W1 and W2. The borehole W2 was left until last because it contained some highly transmissive fractures which, when depressurized, reduced heads within the entire volume of the site. In general the 3 N – S boreholes (N2, N3 and N4) were less transmissive than the 2 E – W boreholes. The total transmissivities of the five boreholes are as follows:

Borehole	Drilled length (m)	Tested interval distance in b/h (m) to (m)	Total borehole transmissivity ($m^2\ sec^{-1}$)	Number of mapped "open" fractures in tested zones
N2	207.1	7.9 – 194.9	$1.6 \cdot 10^{-7}$	219
N3	192.1	8.9 – 182.9	$3.0 \cdot 10^{-8}$	410
N4	220.0	8.0 – 182.9	$4.8 \cdot 10^{-7}$	641
W1	147.3	8.0 – 135.1	$1.9 \cdot 10^{-7}$	578
W2	148.0	7.9 – 140.7	$2.2 \cdot 10^{-6}$	594

The difference between the two orientations of borehole can be seen in two representative plots: boreholes W2 and N4, see Figures 4-14 and 4-15.

The use of the "focussed testing approach" can be clearly seen in the results and the generally higher values associated with W2. Where zones are subdivided there are a commensurate set of results for the "other half" of a subdivided interval. However, it still turned out that there were very few single fracture intervals.

The heads in the two example boreholes are shown in Figures 4-16 and 4-17. Whilst N4 shows the more usual situation where the instrument drift is the major low head affecting the borehole, W2 shows another situation. It appears that a fracture with very low head occurs at the end of borehole W2.

The results from the testing are due to be interpreted in detail for the purposes of network modelling during 1988. This will involve the use of the fracture statistics and varying levels of supposition concerning the distribution of transmissivity.

Other Testing

The equipment has also been used to carry out a number of specific tests on individual fractures for the research programme devised by Tom Doe concerning the estimation of distances to fracture intersections. This work is reported separately.

Summary

A new approach which involves complex equipment has been successfully devised and deployed in the field. Although the approach was devised with the needs of fracture net-

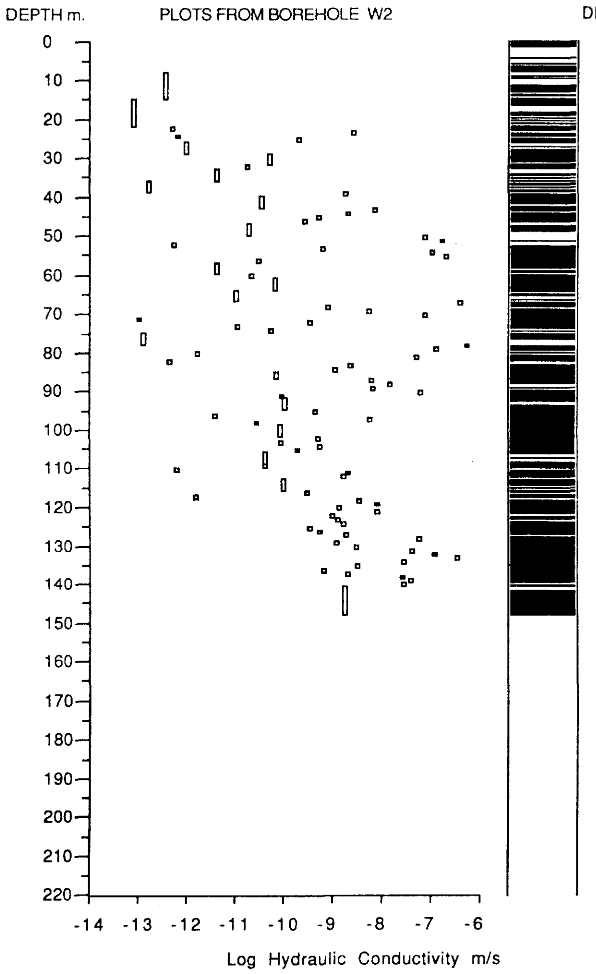

Figure 4-14. The distribution of hydraulic conductivity within the borehole W2 (the right hand column shows the distribution of fractures in the borehole).

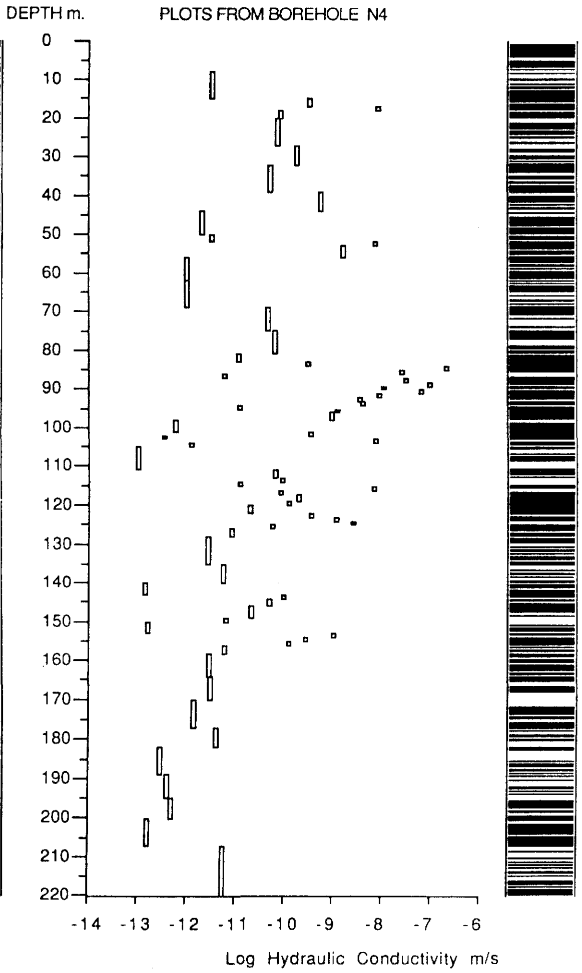

Figure 4-15. The distribution of hydraulic conductivity within the borehole N4 (the right hand column shows the distribution of fractures in the borehole).

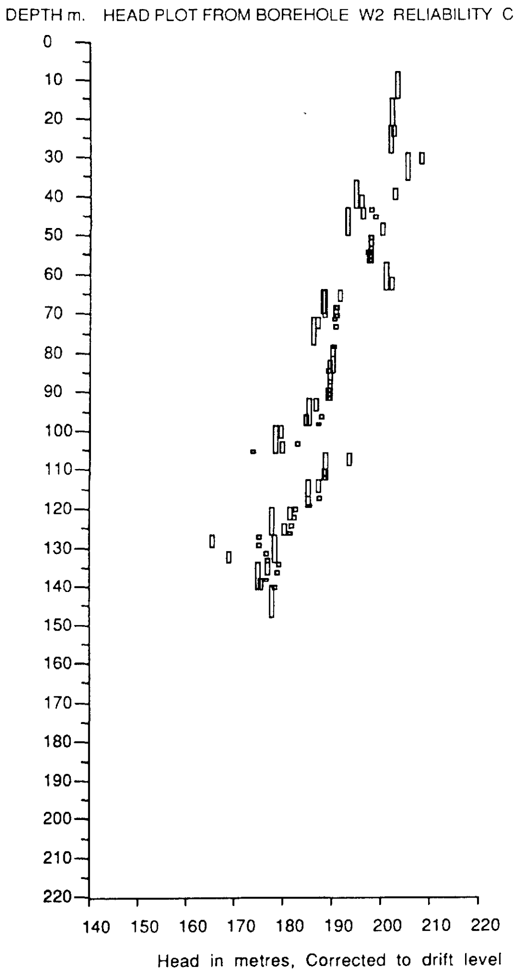

Figure 4-16. The profile of "environmental head" within the borehole W2 relative to drift level.

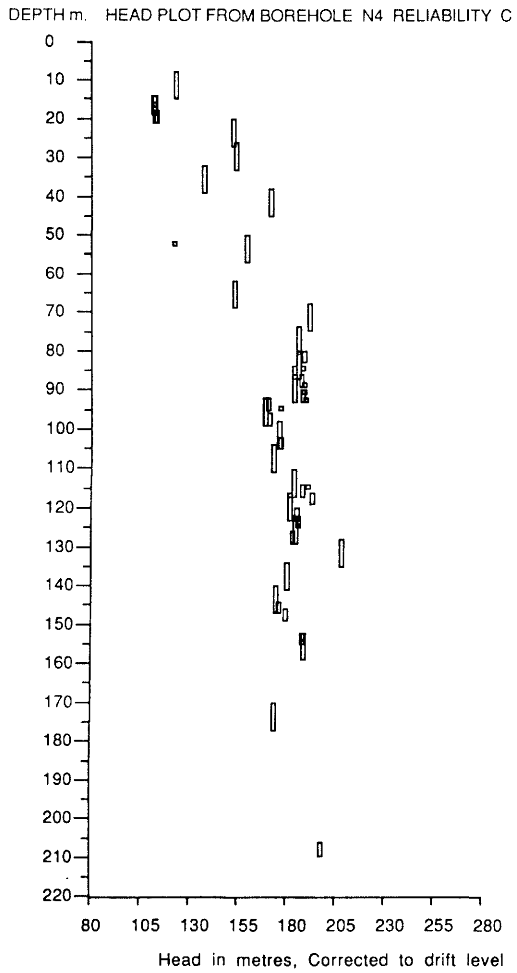

Figure 4-17. The profile of "environmental head" within the borehole N4 relative to drift level.

work modelling in mind, it forms a sound approach to all hydraulic testing. It requires, however, a "high technology" attitude and set of equipment which recoups costs by savings in time or improvements in data. The approach and the equipment enable the speed of testing to be varied with a commensurate variation in the level of accuracy and reliability of the derived results. It represents a significant step forward in the hydraulic testing of single exploratory boreholes.

The results for the testing appear at first examination, to be sufficient for the requirements of the modelling. The results are yet to be analysed in detail.

4.1.7 Fracture Characterization

Fractures in most rock masses exist on a number of distinct but overlapping scales. For the purposes of the present study we are primarily concerned with the regular joints and the fault/shear/fracture zones. The really small scale members of the fracture family such as fissures and microcracks may be important in that they may contribute significantly to the ability of the rock mass to absorb radionuclides but they are not the main focus of this study.

The contribution of a fracture to the transport or permeability properties of a rock mass is determined in part by its dimensions parallel to its plane (its trace length) and by its aperture. Both fracture zones and joints have different but finite trace lengths. If the fracture trace lengths can be observed and mapped the distribution of trace lengths can be characterized by the moments of an appropriate distribution or statistical model. Since fractures have a finite trace length their contribution to the permeability of the rock mass also depends on whether their trace lengths are long enough to be continuous from flow boundary to flow boundary across the rock block or rock mass being investigated. If the trace lengths are shorter than the rock mass dimensions then the contribution of a particular scale of fracturing to the rock mass permeability also depends on how well the fractures are interconnected. At Stripa the trace lengths of the joints are only about one to two percent of the Phase 3 block dimensions. Also, while the length dimensions of the major fracture zones appear to similar to the dimensions of the Phase 3 block they are discontinuous on the scale of the rock mass in which the block is located. Hence the interconnectivity of both scales of fracturing and the cross connection between both scales is a critical factor in determining the transport properties of the Phase 3 block. However, the interconnectivity of a fracture system is a complex expression of the fracture geometry, that is the distribution of fracture orientations, trace lengths and spacings.

In the area of the Phase 3 block as with most underground sites the rock mass available for direct observation is limited to the surface of a limited number of drifts (Figure 4-1) with four different orientations. Because of the similarity in dimensions, these drifts permit the collection of data on the orientation and trace length (and to some extent spacing) of the joints intersecting the drifts. On the other hand, boreholes (Figure 4-1) close to and through the Phase 3 block provide additional information on fracture orientations and spacings, but no additional information on the trace lengths of individual fractures. Thus, boreholes and drifts form complementary data sets that should provide a fairly complete picture of the fracture system in a given rock mass. Hence, as part of the Phase 3 study a systematic program of mapping fractures that cut scanlines along drifts (Figure 4-1) as well as the fractures intersecting the reconstructed and oriented drillcores was carried out in order to characterize the geometry of the fracture system in the Phase 3 block.

Fracture Data from Drift Mapping

Fractures intersecting seven individual scanlines were systematically mapped as part of the Stage 1 Site Characterization program. Scanlines 1 and 3 are located along the access drift to the 3-D Migration test area, scanline number 2 runs the length of the inclined drift leading from the Extensometer drift, where borehole N4 is located, to the 360 m level and scanlines 4, 5, 6 and 7 are located in the 3-D Migration test area. Basic data were collected

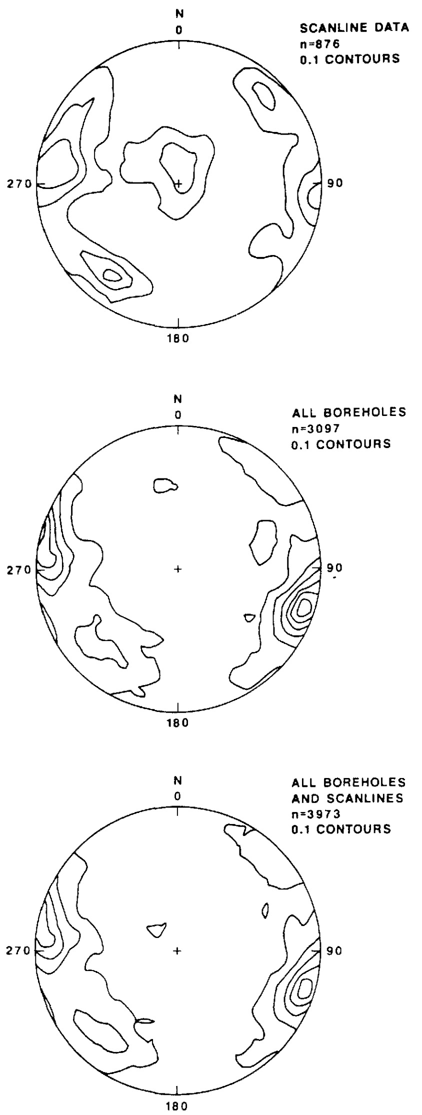

Figure 4-18. Lower hemisphere plots of poles to fracture planes.

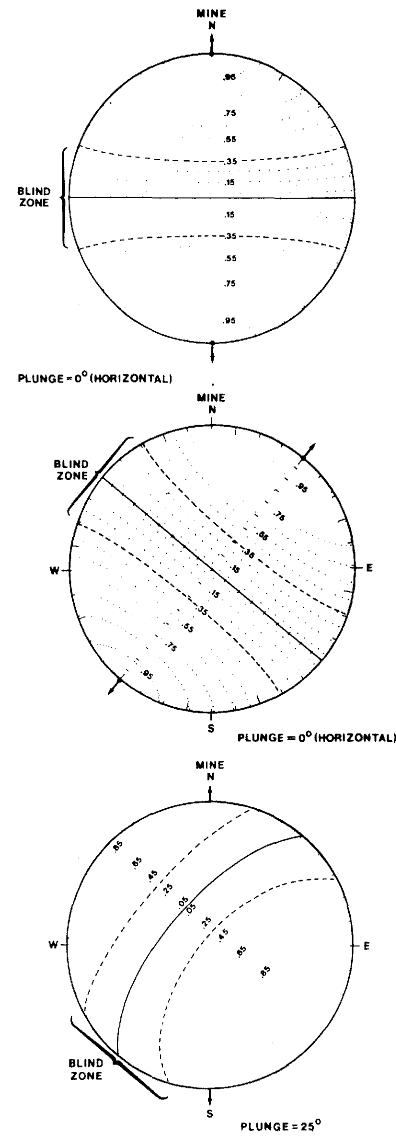

Figure 4-19. Orientation bias or blind zones associated with each drift or scanline orientation.

on fracture orientation, trace length, termination mode, surface characteristics and fracture filling minerals. In addition, a number of fractures that did not intersect the scanlines were mapped.

The lower hemisphere contour plot of the density of poles to all of the fracture planes measured along the drift is given in Figure 4-18. The values being contoured represent densities calculated by weight the density at each point by the angular distance from each of the poles from the point in question. The first plot in Figure 4-18 has been constructed from both the fractures intersecting the scanlines and those intersecting the drift walls, but not the scanlines, on which the scanlines were measured. Three fracture sets have been tentatively identified from the clusters defined by the density contours. These sets, while slightly rotated, appear to correspond to sets 1, 2 and 4 from the Buffer Mass Test area as labelled in the earlier report by Gale and Rouleau (TR-86-05) and the same set numbers have been applied here for consistency.

The orientation of the drifts and hence the scanlines introduce an orientation bias (Figure 4-19) to the plot of poles to fracture planes (See paper by R. Terzaghi, 1965; Sources of error in joint surveys, Geotechnique, v. 15, pp. 287-304). Here we arbitrarily assume that any fracture plane that intersects a scanline or borehole at an angle of $\leq 20^0$ will not be adequately sampled by that borehole or scanline.

Fracture Data from Boreholes

The orientation of fractures intersecting the drillcore from boreholes N2, N3, N4, W1 and W2 were determined by reconstructing the core and measuring the relative dip (alpha) and dip direction (beta) with respect to a reference line that was drawn on each reconstructed section. The true orientation of a well defined fracture in each reconstructed section was determined using either televiewer or borehole TV camera surveys and used to determine the orientation of a reference line connecting the lowest points on the core. Using the orientation of the reference line and the relative orientation angles the true dip and dip direction for each fracture were calculated. Approximately 95% of the cored sections were oriented using either the televiewer or TV camera surveys.

The contour plots of poles to sealed and coated fracture planes for the N and W boreholes are given in Figures 4-20 and 4-21, respectively. Boreholes N2, N3 and N4 plunge 18.6 degrees, and W1 and W2 plunge 5 degrees, parallel and perpendicular to Mine North, respectively. The number (n) of individual fractures is given in each pole diagram. The contour lines are spaced at 0.1 intervals with the first contour line starting at 0.1 contour level.

The N boreholes, because of their steeper plunge and hence greater vertical span, intersect a greater percentage of sub-horizontal fractures than the two W boreholes as shown by the contour lines on the pole diagram for each borehole. However, the sub-horizontal fracture planes are oriented sub-parallel to both the N and W boreholes and hence lie within what is generally described as the "blind zone" on the stereographic plot. Thus, the N boreholes should provide a good sample of any East-West trending sub-vertical fracture set and the W boreholes should provide a good sample of any North-South trending sub-vertical fracture set if these sets are present in the rock mass.

Comparison of the contour plots in Figures 4-20 and 4-21 shows that the W boreholes have intersected a strong North-South trending sub-vertical fracture set. However, the N boreholes do not indicate the presence of strong East-West trending sub-vertical set. Instead the N boreholes show pole clusters in the NE, NW, SE and SW sections of the pole diagrams. These clusters may be part of the East-West trending distributions. When we combine the 3097 poles from the N and W boreholes (Figure 4-18) the East-West clusters dominate the contour diagram. However a considerable amount of background data is lost due to the dominance of the East-West cluster. The data from the scanlines (Figure 4-18) indicate two sub-vertical fracture sets and a sub-horizontal fracture set. When the borehole and scanline data are combined (Figure 4-18) the relative strength of the sub-horizontal set is greatly diminished, indicating the danger of using contour plots of pole densities to define sets or clusters when one does not have an equal number of fractures from each set.

Discussion

Prediction of fracture geometry over rock masses the size of the Phase 3 block requires a measure of the spatial variability of the fracture geometry. As an initial analysis of the spatial variability of the fracture geometry within the Phase 3 block we have constructed pole plots for each 50 m increment of the five boreholes (Figures 4-22 and 4-23). The individual pole plots are shown in their correct relative position. Since these borehole plots contain significant orientation bias, we have combined 60 fractures from each of two boreholes at their points of intersection. Although the two boreholes are separated vertically, they do provide two sampling directions at six points (Figure 4-24) within the rock mass. From these different pole plots it can be seen that the fracture orientations do vary over the Phase 3 block. In order to develop the conceptual model for the fracture geometry within the Phase 3 block, we will attempt to quantify this variability and determine if fracture density

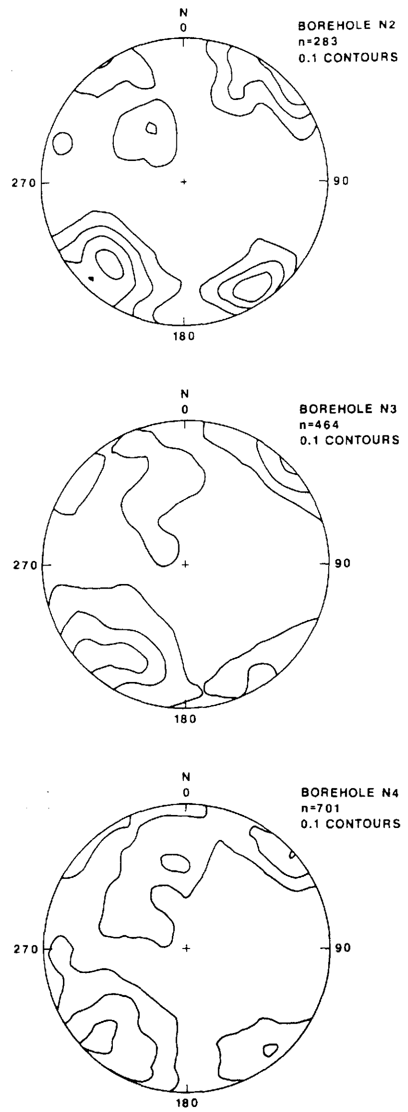

Figure 4-20. Lower hemisphere plot of poles to fracture planes (sealed and coated) for each of the three N boreholes.

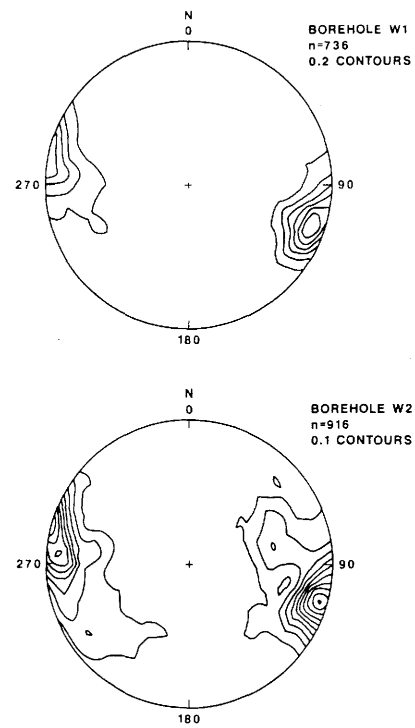

Figure 4-21. Lower hemisphere plot of poles to fracture planes (sealed and coated) for each of the two W boreholes.

also varies significantly within the Phase 3 block. Hence considerable efforts will be devoted to determining the parameters of the statistical models that best fit the orientation, trace length and spacing distributions for the combined data set from the drift and boreholes in the Phase III block.

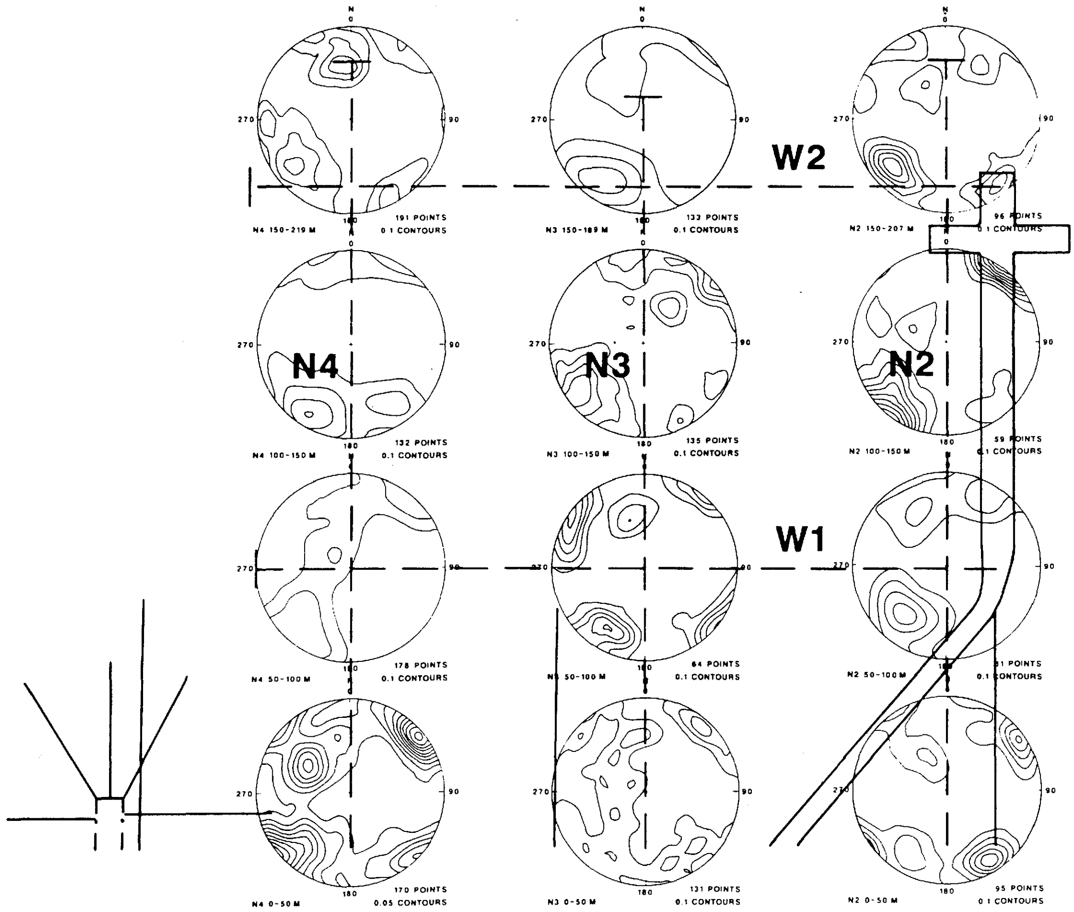

Figure 4-22. Lower hemisphere pole plots for each 50 m section of the N boreholes.

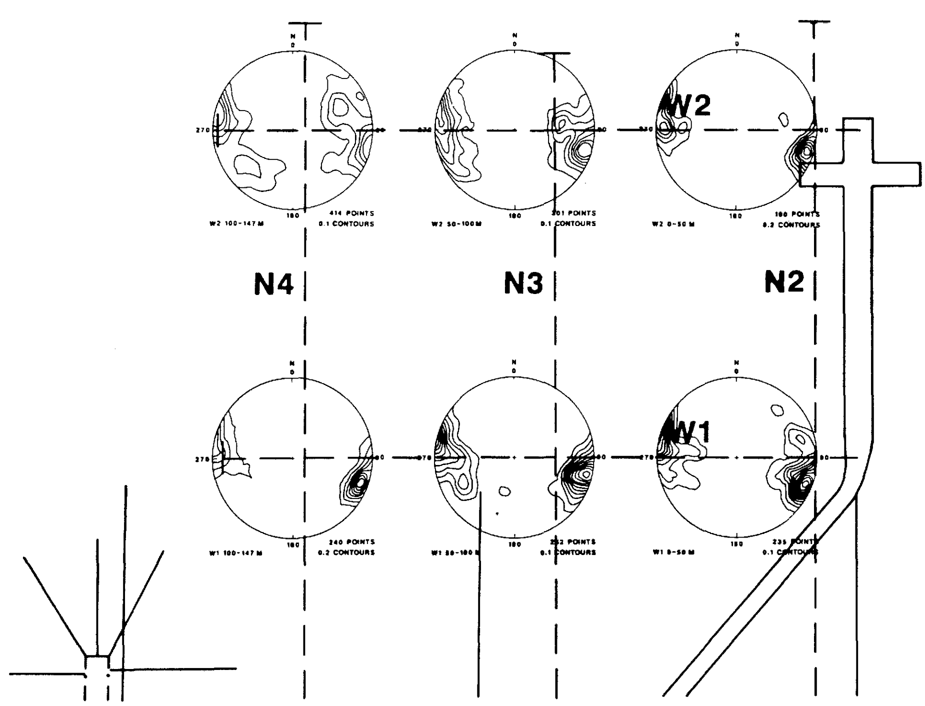

Figure 4-23. Lower hemisphere pole plots for each 50 m section of the W boreholes.

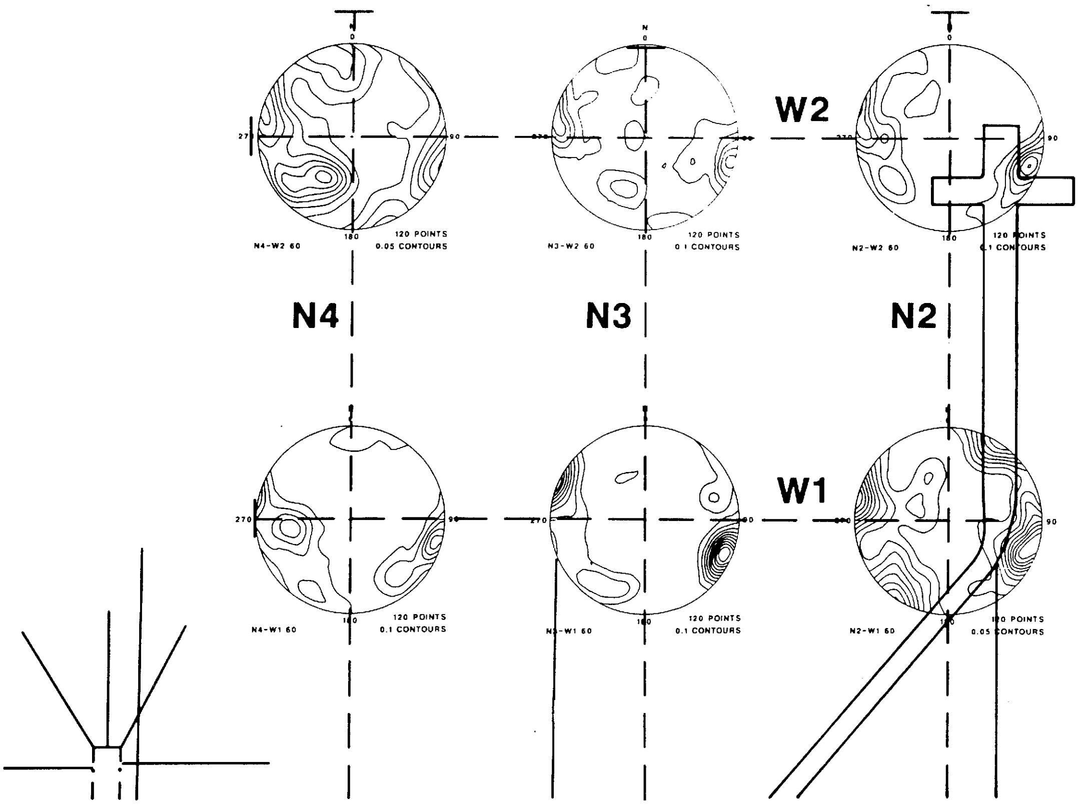

Figure 4-24. Lower hemisphere poleplots for 60 fractures from each of the N and W boreholes at the points of intersection.

4.1.8 Hydrochemical Investigations in the Site Characterization and Validation Task of Phase 3

The chemical composition of the groundwater sampled in the conductive parts of the newly drilled holes N2, N3, N4, W1 and W2 is used to locate different flow paths in the investigated rock mass. Based on the composition it is also possible to judge whether the groundwaters are recently mixed due to e.g. short-circuiting of different flow paths through the boreholes.

Since September 1987 water samples have been collected and analyzed from the N and W boreholes. A mobile field laboratory has been used for the analyses of main components and redox sensitive trace elements. This laboratory has been lent by the SKB for the performance of these investigations.

Based on the results of the hydraulic tests suitable sampling sections have been located. In total 19 water conducting sections have been sampled.

Based on the composition these can be devided into a saline group A and a non saline group B. The saline group can be further devided into the subgroups A1 and A2. The classification of the waters are given in Table 4-3.

Table 4-3. The classification of the sampled groundwaters.

Group	Cl/mg/l	HCO_3/mg/l	Na/mg/l	Ca/mg/l	pH
A2 (N2:137)	230	15	110	48	9.4
(N2: 95)	170	27	110	27	9.6
A1 (N2:152, N3)	130(10)	50(3)	70(5)	30(2)	8.7(1)
B (N4, W1, W2)	40(10)	90(10)	45(5)	18(3)	8.6(2)

The waters sampled from the conducting sections of the boreholes N2, N3, N4, W1 and W2 are of two types, saline and non saline. The saline waters are encountered in N2 and N3. These constitutes a flow regime which is separated from the one of the boreholes N4, W1 and W2.

Evidently there are hydraulic connections between the conducting sections of W1, W2, and N4:16, 49, 84 m.

4.2 DEVELOPMENT OF HIGH RESOLUTION AND DIRECTIONAL RADAR

4.2.1 Introduction

The borehole radar developed during Phase 2 has a demonstrated ability to detect fracture zones in different geological environments. Radar measurements can also with considerable accuracy determine the angle of intersection between a fracture plane and a borehole. The antennas are, however, axially symmetric with respect to the borehole and this makes it physically impossible to determine completely the orientation of a reflector. Such information has rather been obtained by combining results from several boreholes during the analysis of radar data.

It would be very valuable to obtain the missing angle (the azimuth) directly during measurements in a single borehole. Radar measurements could then be performed efficiently at sites where only one borehole is available. Furthermore the identification of individual fracture zones would be simplified if all the necessary data were available in the original radar picture.

The principles of a directional antenna are easy to describe but there are a number of practical decisions that must be tested in order to construct a reliable instrument. The numerical analysis of radar data must also be adapted to the increased data flow which will require new methods of computation and display. Finally the instrument must be tested on real fracture zones which are often quite different from simple planes as demonstrated in the radar work performed during Phase 2.

4.2.2 Principles of Construction

Directional information can be obtained by displacing the antenna elements from each other in the direction corresponding to the measured angle. This is easily done for directions along the borehole and consequently the angle of intersection of a fracture plane with a borehole can be accurately determined. In the other directions we are limited by the diameter of the borehole which is always much smaller than the wavelength of the radar waves. One is thus more or less restricted to construct an oblong loop antenna with quite low radiation efficiency and poor angular resolution. This is, however, not a serious disadvantage as long as one is trying to determine the position of an object which has already been identified, for instance in other radar pictures.

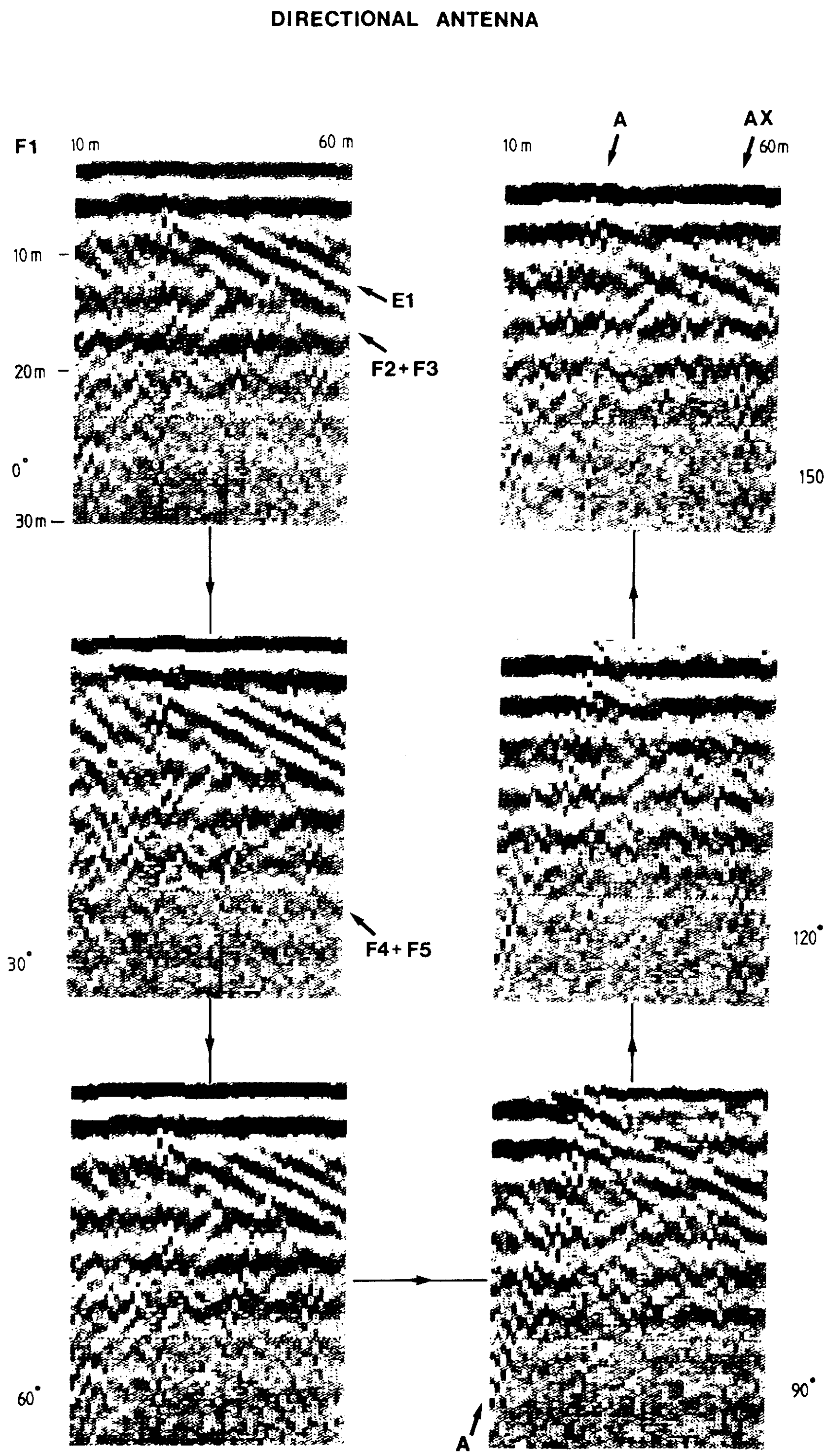

Figure 4-25. Measurements with a loop antenna demonstrating the rotation of a directional antenna in 30° steps. Measurement performed between 10–60 m in borehole F1 in Stripa. The reflectors are well known fracture zones and boreholes identified by letters.

The basic principle of the directional antenna was tested in detail in Stripa using several different experimental loops which were rotated by hand in the boreholes. The results proved successful: the basic physical parameters agreed with theory and it was possible to imitate a real measurement to about 60 m depth in one of the boreholes as shown in Figure 4-25. It is clearly seen how the various reflectors (fracture zones and other boreholes) disappear and reappear when the antenna is rotated in the borehole. A rotation through 90° will bring the signal strength from a maximum to a minimum.

The most difficult problem is to decide how the antenna should be rotated in the borehole. A motor may be used to turn the loop mechanically. We have, however, decided to test an electronically rotated antenna avoiding moving parts in the construction. There are then switches connecting the different antennas in turn to the receiver. The disadvantage of such a system is that it must be carefully calibrated since the different signals cannot otherwise be added in a meaningful way. For instance, omnidirectional electric dipole components will always appear due to imperfect balancing of the antenna feeds. These fields must be eliminated during the analysis of the data in order to obtain the correct azimuth of the reflector.

The directional antenna has been constructed as an extension of the existing system and the following items have been added:

1) An rotation indicator which gives continuous information about the orientation of the antenna in the borehole;
2) A fourth optical fibre communicating both ways with the rotation indicator and the antenna switches;
3) An antenna which provides four different signals containing directional information about the reflectors;
4) An extension of the radar program for collecting, analyzing and displaying directional radar data.

The receiver has been considerably improved by new amplifiers and a new sampler which can handle the increased frequencies required by the directional antenna as well as other high resolution antennas foreseen within the program.

A first test of the radar system took place in Stripa where a number of calibration measurements were performed. The analysis showed that the measured signal can be separated into directional and dipole components in the way predicted by theory. The error is quite small as shown in Figure 4-26, where the least square deviation has been indicated with the signals.

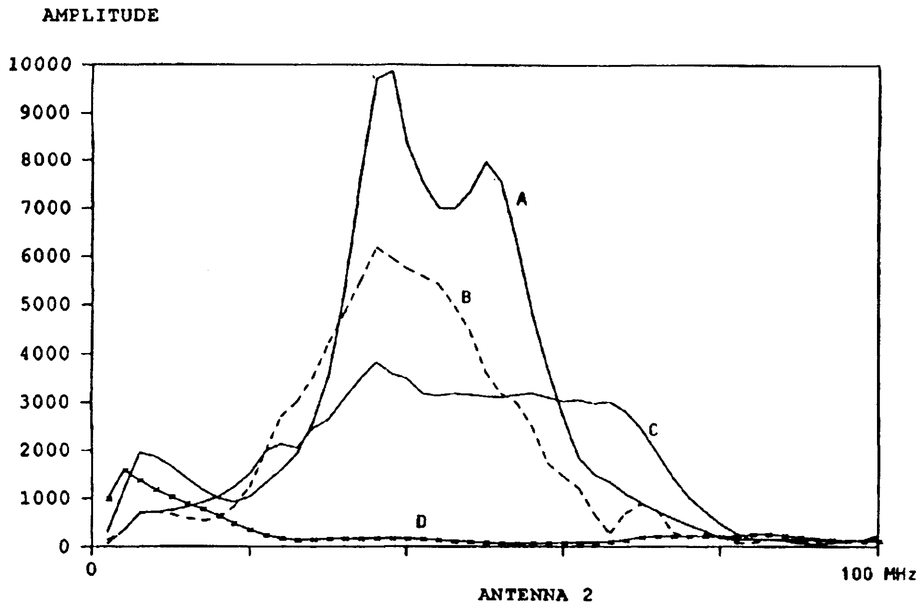

Figure 4-26. The frequency spectrum of a radar signal separated into an electric dipole field (A) and two directional components (B and C). The remaining error (D) is small demonstrating that the results agree with theory. The noise at low frequencies is generated by the amplifier.

The signals from different antennas were, however, not quite similar in spite of the assumed symmetry of the antenna elements. Several possible reasons for this asymmetry were investigated and it was deduced that there must be a short between some wires. This was confirmed in new measurements in the lab where the antenna finally became perfectly symmetric. Poor connections are difficult to detect since they often appear during transport or when the probes are opened or closed. Some tests will therefore be included in the future radar program to test the symmetry of the antenna system both during measurements and calibration.

4.3 IMPROVEMENT OF TECHNIQUES FOR HIGH RESOLUTION BOREHOLE SEISMICS

The tasks for the year 1987 were:

- the construction and testing of a prototype coherent seismic source,
- development of algorithms and programs for processing the waveform information and
- the construction of a field acquisition/processing workstation for quick result interpretation on site.

The construction of the prototype source and of the field workstation were completed during 1987 as planned. The work on the software has proceeded so far with good results.

4.3.1 The Coherent Source

First, a conceptual design of a piezoelectric source was done and it became apparent that the source should be able to output coherent bursts as an alternative to long monofrequent wave-trains. The wave-trains lead to ambiguous seismic velocity determination thus losing information needed by the processing techniques already in use (e.g. tomography).

A set of tests with piezo elements as seismic sources were performed during April. The equipment used was laboratorylike and consisted of:

- Waveform generator (adjustable freq. and wavetrain length) – Power amplifier (50 VA max.)
- Piezo source (natural freq. in water: 7 kHz)
- 2 hydrophones
- Digital oscilloscope (4 channel, 10 microsec. sampling)

The character of the coherent burst did not change after travelling through rock, the seismogram being a sequence of tapered wavelets similar to the source signature. It is thus possible to include the waveform information in the interpretation.

Due to the low power used, the quality of individual records was not very high for ranges over 15 m but the noise has practically vanished after 200 stacks and narrow band pass. The tests showed that, if properly designed, this kind of source is suitable for small scale tests (range 50 to 200 m).

Based on the result of the tests, the actual source prototype was constructed (Figure 4-27), with a significantly higher output level. The power of the amplifier used to drive the source was also increased from 50 VA to 2000 VA.

4.3.2 The Field Acquisition/processing Workstation

The data acquisition/processing unit was built by fitting a 16-channel analog/digital I/O module to a microcomputer. The computer was chosen to have field operation capability (Figure 4-28). The data is primarily stored on hard disk and a cassette backup is provided.

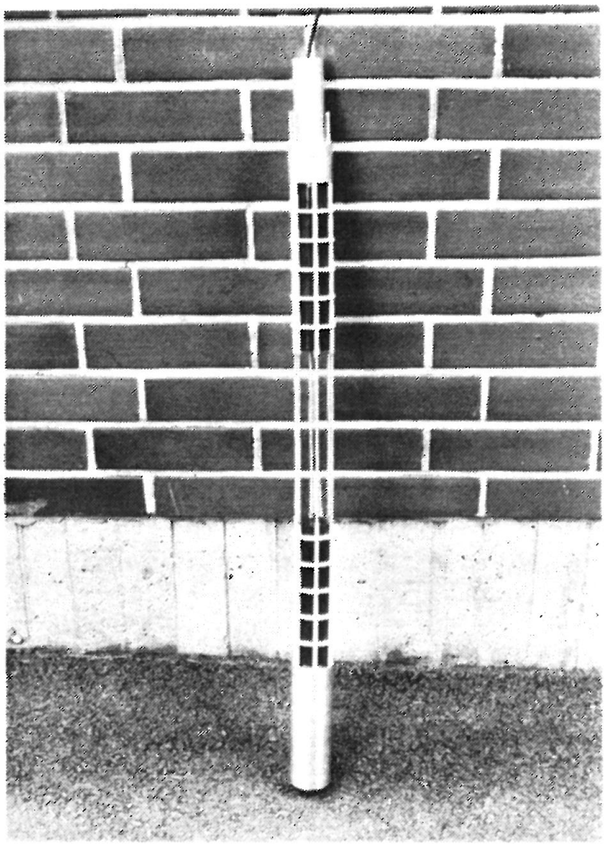

Figure 4-27. Prototype of a coherent seismic source.

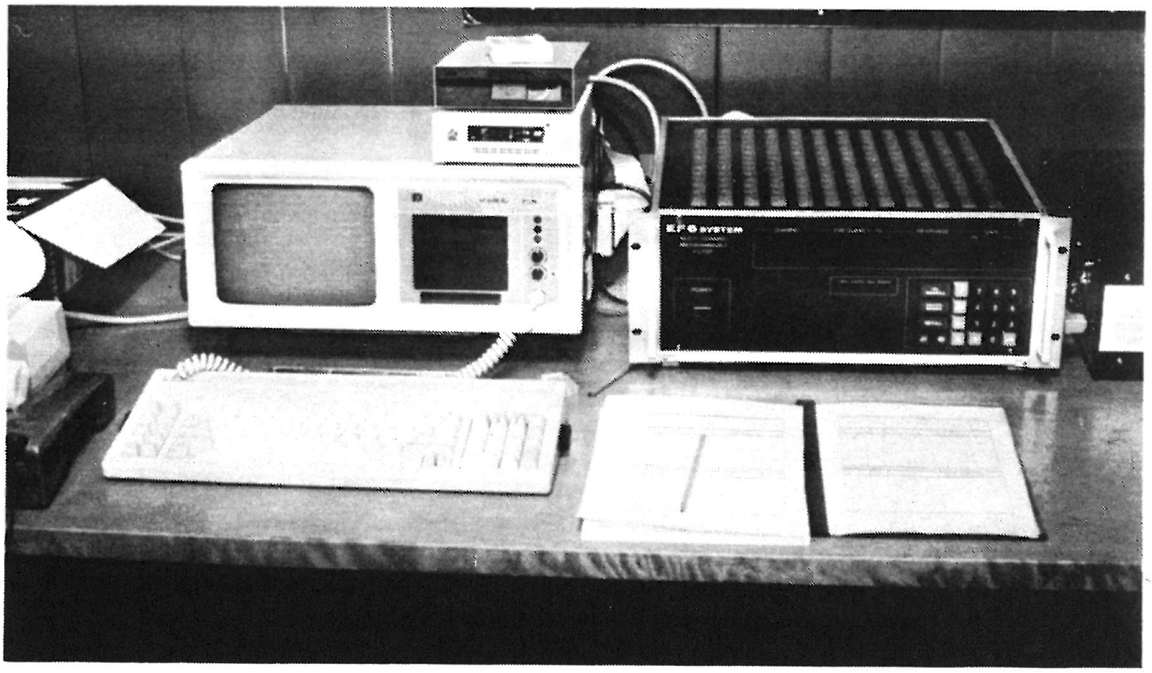

Figure 4-28.
Left — field microcomputer
Right — filters/amplifiers bank

The A/D converter has a resolution of 12 bits. The maximum sampling rate is 1 000 000 samples per second.

The filters/amplifiers form a 16-channel bank and they can be interconnected for bandpass and band reject responses (Figure 4-28). The amplification is done in two steps, pre and post filtering on each channel. The gain can be set from 1 to 64 in steps of 1 for both amplification steps. The filters can be selected as high or low pass from 0 Hz to 100 kHz in five ranges, the step varying from 0.1 Hz for the lowest range to 10 Hz for the highest. The filters have a slope of 178 dB per octave with options for response linearization.

4.3.3 Processing and Interpretation Routines

With the software development, the efforts were directed to connecting different procedures from data acquisition to final interpretation and presentation of results. As a consequence, less emphasis was placed on the theoretical topics like acoustic holography and migration techniques and more on their application in velocity filtering and three-dimensional interpretation of structures. The starting point was the work performed in the Second Phase of the Project.

The novelty of the interpretation procedures developed lies in the efficiency of the filtering in two dimensions (time and depth) of the sets of seismograms and in the way of calculating the geometry of the reflectors.

The two-dimensional filtering leads to the enhancement of the events which are coherent over large regions of the timedepth profiles. We have used a variant of a non-linear filtering method. This method is based on the P-Tau Transform. The main advantage of this approach is that in the transformed section events with different velocities will appear separated on different traces. In this way the P-Tau Transform can be used for example to separate the upgoing and the downgoing events. It is equally possible to design more elaborated filter functions which will enhance curved events like the ones expected from inclined reflectors.

The next step in the interpretation procedure attempts the construction of a geometrical model consistent with the position and shape of the reflected events observed in several profiles. From only one profile both the dip and the strike of a reflector cannot be determined independently. Therefore, the reflector position cannot be determined from its trace in a single profile. If the same reflector is identified in more profiles, its position in three dimensions can be calculated.

Some difficulty has been experienced so far with the identification of the same reflector in more profiles. This happened because the density of reflectors in crystalline rock is relatively large and the planarity assumption is not always applicable.

4.3.4 Tests with the Coherent Source

Tests with the coherent source were performed in the N2 and N3 boreholes at the SCV site in the Stripa mine during February 88.

Frequencies up to 10 kHz were tried with excellent signal transmission. The frequency was then fixed to 6000 Hz. The source was moved at 1 m increment in N3 between 50 and 100 m.

A detector of the triaxial accelerometric type was kept in a fixed position at 50 m depth in N2. The number of stacks added for the same record varied from 300 to 500 at a rate of 10 stacks per second. A sampling frequency of 50 kHz was used and the signals were bandpass filtered between 2 000 and 10 000 Hz. All the energy in the seismograms was concentrated as expected around 6000 Hz in a very sharp peak (Figure 4-29).

The seismograms show indications of strong later onsets (reflections) from the major features crossing the site as well as from tunnels and shafts (Figure 4-30). Some of the reflectors detected were more than 200 m away. The 2-way signal travel, i.e. the range of the instrument, is then close to 500 m (Figure 4-31).

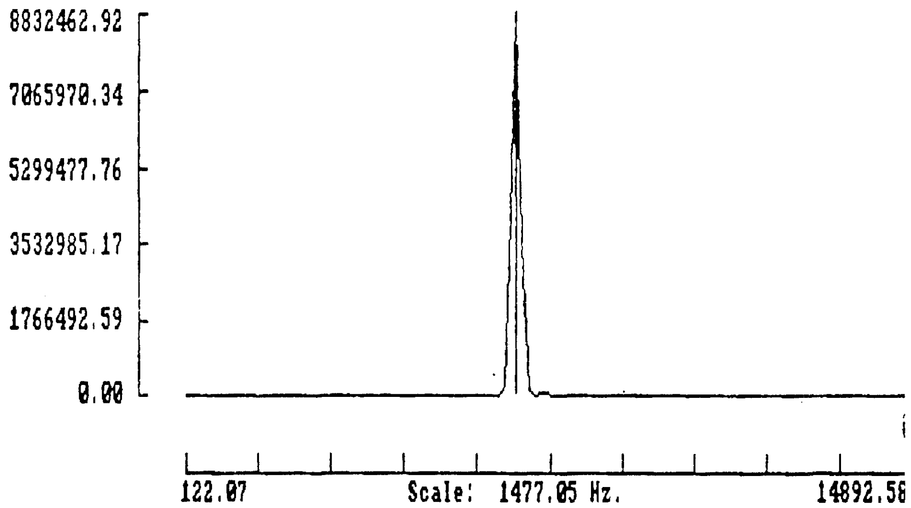

Figure 4-29. Amplitude spectrum of seismogram recorded from coherent source at 6000 Hz.

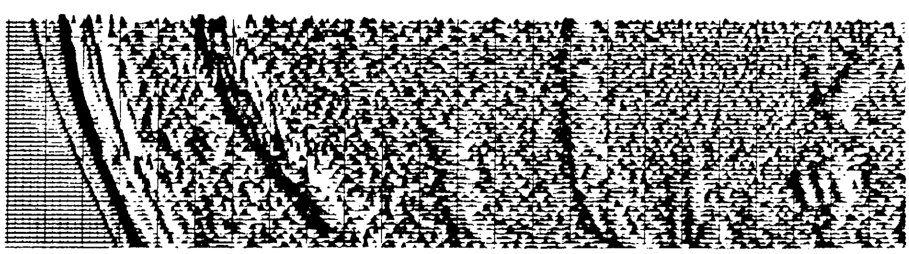

Figure 4-30. Crosshole reflection profile between N3 and N2. Strong events are seen from more than 200 m away.

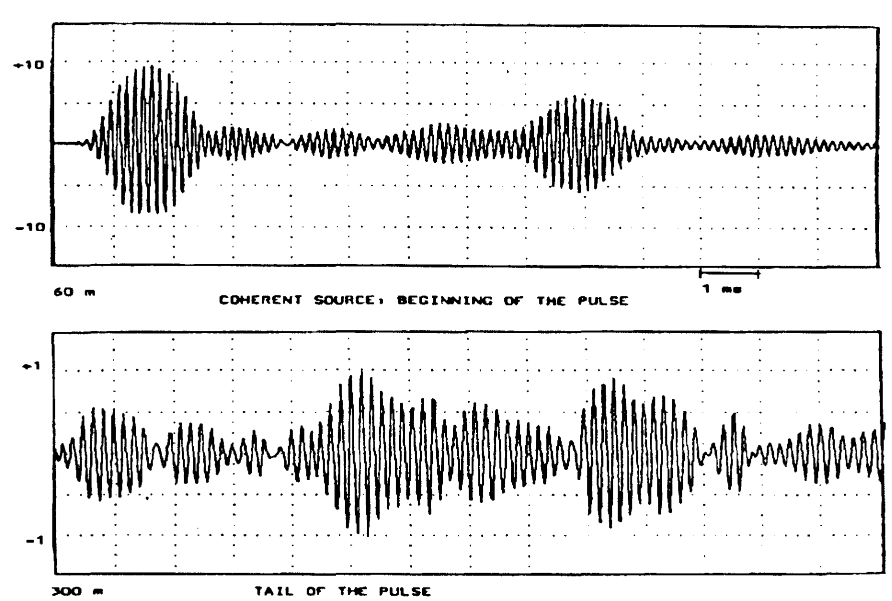

Figure 4-31.
Up — Beginning of seismogram showing events from 60 to 160 m signal travel.
Down — Tail of seismogram showing events from 300 to 400 m signal travel.

4.3.5 Tests of the Interpretation Techniques

The processing and interpretation routines have been tested on data collected at the SCV site during Phase 1 of the Project.

Two locations in the drift, Pl (near the top of borehole W2) and P2 (near the top of borehole Wl), were used in the reflection analysis. The signals from Pl were recorded in both holes resulting in a zero offset VSP-like section for borehole W2 and a 70 m offset section for borehole Wl.

Mechanical shocks were produced at these two points by means of a sledge hammer. The receiving units were 3-D accelerometers. Although the sledge hammer is not an appropriate source for reflection surveys due to the instability of the signal shape, the test proved that the techniques developed within this project are usable for detection of reflections from fractured zones in crystalline rock and for computing the position of the reflectors (Figures 4-32 to 4-34).

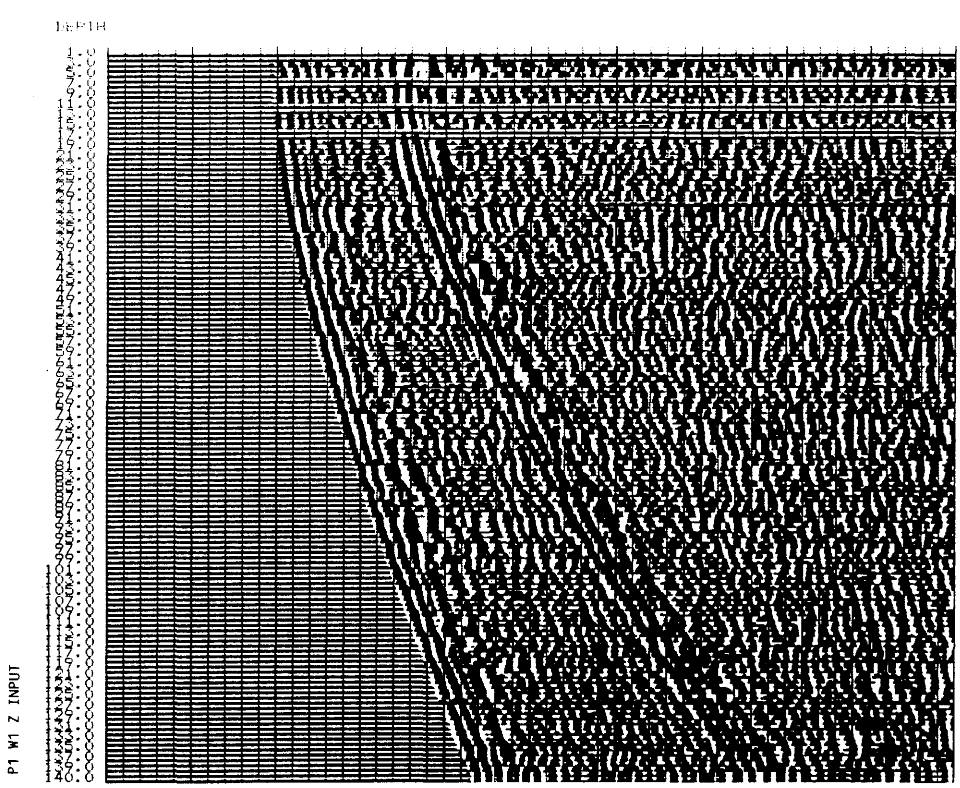

Figure 4-32. Reflection profile obtained by sledge hammer blows in the drift (filtered and deconvolved).

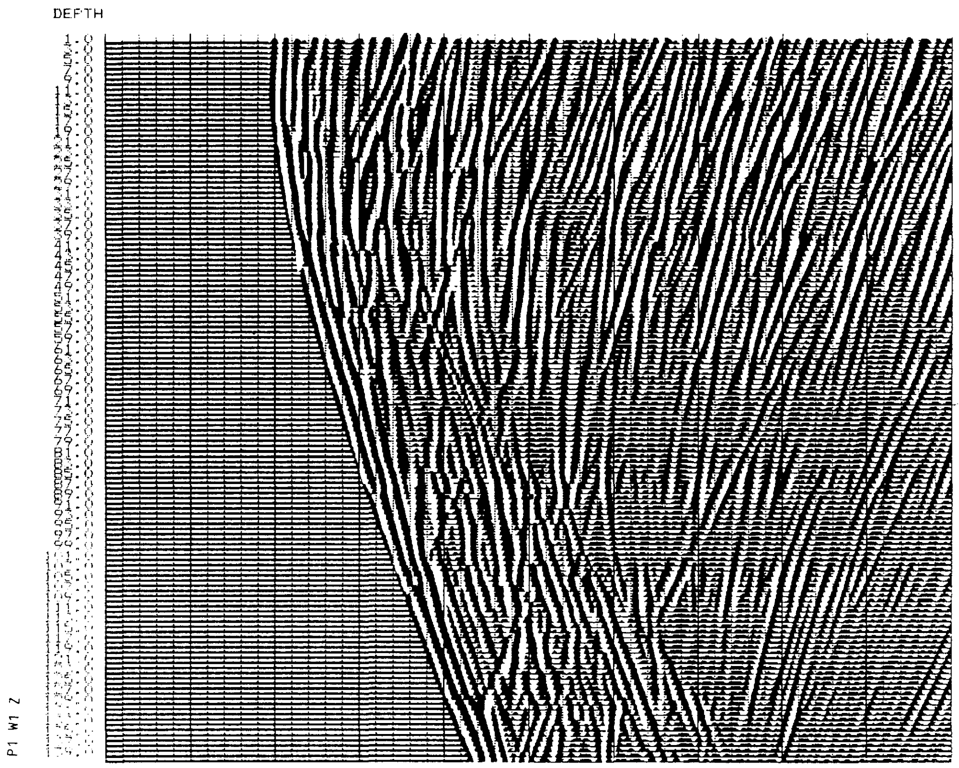

Figure 4-33. Reflection profile from Figure 4-32 after Tau-P filtering. Many reflected events (inclined to the right) are visible.

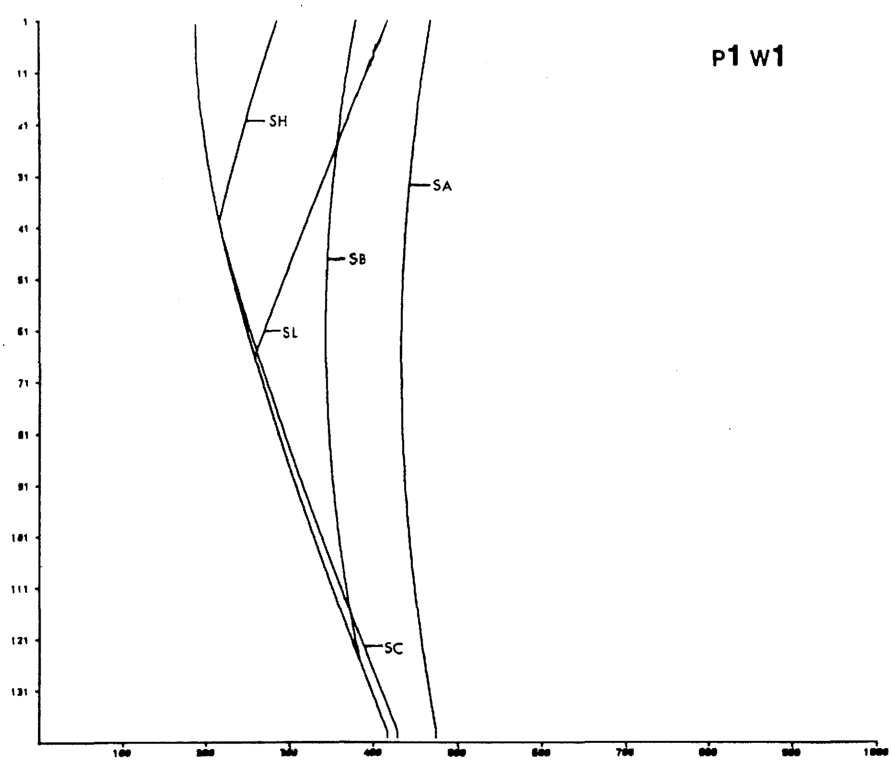

Figure 4-34. Identification of major features inferred from the reflection profiles after calculating their orientation in 3 dimensions.

4.4 FRACTURE NETWORK MODELLING

4.4.1 General

The disused mine at Stripa provides access to fractured rock of a kind that might accommodate a repository for nuclear waste. The assessment of any repository located beneath the water table relies upon predictions of groundwater flow and radionuclide transport therein. Flow through fractured rock is predominantly along distinct and widely spaced fissures. Hence fractured rock should be approximated as a continuous porous medium only in simulations that deal with large volumes of rock containing many fissures. Moreover, only observations on a substantial scale can fix appropriate values for the parameters in such continuum models. Experiments to determine directly the equivalent permeability or dispersivity of fractured rock are therefore inevitably both expensive and time-consuming.

An alternative approach is to calculate flow through networks of distinct fissures. The actual rock is represented by a set of realizations with the measured fracture density, that are generated by sampling distributions of the length, transmissivity and orientation of the observed fissures. Such stochastic fracture network modelling predicts a distribution for the results of measurements of flow within the rock. Network simulation also establishes explicit criteria for the application to fractured rock of equivalent porous-medium models. Where such models are appropriate, the relevant parameters may be determined by appropriate network calculations. Hence network simulations can in principle calibrate equivalent porous medium models of fissured rock against local observations of fracture length, density, aperture and orientation; whereas direct calibration of such continuum models requires expensive and time-consuming global measurements.

Phase 3 of the Stripa Project aims to develop and demonstrate tools for the assessment of sites for repositories to contain radioactive waste. The Project has therefore funded the further development of the Harwell three-dimensional network code, named NAPSAC. In Stage 4 of the present phase of the project, the code will be involved in predicting flow into the validation drift.

4.4.2 Development of the NAPSAC Code

Architecture

Continuum calculations of groundwater flow often exploit finite elements that cover the entire domain. The pressure field is approximated by a sum over terms each proportional to a basis function localized at a node; each node is situated either on the edge of an element or at a particular point in the interior, so that the basis functions have simple forms. The equations determining the coefficients of the basis functions result from imposing conservation of fluid. The equations are linear if flux is proportional to the pressure gradient.

Network simulations are in some sense finite-element calculations; however, the basis functions are now localized about nodes spaced along the fracture intersections. Over a single fracture, such a basis function has unit value at one node, is zero at all other nodes, and has zero normal gradient at the fracture boundaries to ensure zero flux. Such basis functions must be calculated numerically, except for fractures of very regular shape.

Calculation of Fracture Basis Functions

The NAPSAC code admits rectangular fractures, which are covered by a regular finite-element grid in order to determine the fracture basis functions. To this end, intersections are represented by line sources or sinks following a continuous jagged path along element boundaries. This path approximates the length and orientation of an actual intersection. This approach provides an opportunity for varying the aperture across the fracture, and hence for examining the impact of confining flow to particular channels.

Capability of the NAPSAC Code

During 1987 the NAPSAC code has been progressively enhanced so that it can now calculate flow through a few thousand rather than a few dozen fractures. Such calculations call for very efficient numerical algorithms and a computer with very large memory. In the summer Harwell took delivery of a CRAY2 computer; parts of the NAPSAC code had to be revised to make best use of this resource and to cope with the different operating system. The innermost parts of the code have now been written in CRAY2 Assembler Language, and are executed at over 300 million floating-point operations per second. Calculations with networks of several thousand fractures require only a few minutes.

Networks generated by placing fractures at random, and by sampling prescribed distributions of length, orientation and aperture, regularly exhibit almost coincident intersections, or some other troublesome feature. Much effort has been invested in ensuring that the NAPSAC code copes competently with such challenges.

Verification of Network Codes

Dr. Dershowitz of Golder Associates, who leads one of the two American teams providing additional modelling effort to the Stripa project, has developed an equivalent network code. His approach is, however, somewhat different so that a comparison of results will not only identify gross mistakes but also indicate the impact of different approximations. Solutions to simple test problems suggest that neither code has serious flaws but detailed differences point to opportunities for improving accuracy. Because network modelling relies upon multiple realizations each containing many fractures, random errors are much less significant than systematic errors.

4.4.3 Application of Network Modelling

Scope of Network Calculations

The block chosen for the Phase 3 experiments apparently contains several million fractures, although few seem to carry significant flow. Hence a feasible network simulation of the entire block must ignore fissures with aperture less than a certain size. If the limit is set so that the Phase 3 block would contain no more than a few thousand transmissive fractures, then preliminary calculations suggest that the truncated network will carry about 80% of the predicted flow through a network comprising all observed fissures.

Boundary Conditions

The excavation of the drift is likely to lower the hydraulic head over the surface of the Phase 3 block. Changes at this surface can be calculated by means of an equivalent porous medium model of the vicinity of the mine. The model being prepared for this purpose is consistent with local and regional finite-element models developed to investigate flow in the area surrounding the Stripa site.

The conceptual model in preparation will seek to locate major fracture zones within the Phase 3 block. If the hydraulic impact of these zones can be established, they may provide natural boundaries for detailed modelling within a more restricted part of the block.

Disturbed Zone

Drainage into the validation drift may be markedly influenced by the damaged zone created during excavation. We are reviewing how to account for changes in aperture due to stress relaxation at the drift surface.

4.5 CHANNELLING EXPERIMENT

4.5.1 Background

Model calculations show that channelling may have a strong detrimental effect on radionuclide transport because fast channels may carry some of the mass of the nuclides considerably faster than the average flow would and may give this portion less time to decay. Channelling further aggravates the retardation of sorbing nuclides because less surface area for sorption is available in a channel within a fracture than if the whole fracture surface area is exposed to the flowing water.

4.5.2 Purpose

The objectives of the experiment are:

- o To study channelling properties within single fractures.
- o To study interconnection and mixing between channels within a single fracture.

The channelling properties of interest are:

1. Frequency of channels.
2. Widths of channels.
3. Distances between channels.
4. Fracture transmissivity variations in the fracture plane.
5. Interconnection of channels within a fracture.
6. Mixing between channels.
7. Fracture aperture.
8. Dispersion.

Properties 1 – 4 will be studied in the single hole experiment, where up to 10 holes in different fractures will be investigated. This experiment will give the properties close to the measuring hole.

The interconnection and mixing between channels, fracture aperture and dispersion will be studied in one selected fracture, which previously has been investigated with a single hole test. A second measuring hole will be drilled at a 1 to 2 m distance. Pressure pulse tests as well as tracer injections will be utilized in the double hole experiment.

4.5.3 Experimental Design

Single fractures were investigated in the Stripa Project Phase 1 experiment "Migration in a Single Fracture" by drilling a number of holes perpendicular to the fracture plane, see Figure 4-35. Each hole will with this method just penetrate a minor part of the fracture. Large diameter holes (Ø 200 mm) were in that experiment drilled along the fracture plane from the sampling points in the drift to the injection point about 5 m above the drift in order to determine the concentrations of the sorbing tracers. Based from the experience of drilling along a single fracture plane it was presumed that one could perform channelling experiments where holes with lengths up to at least 2 m were drilled along a single fracture plane.

The experimental layout of the single hole experiments in the "Channelling Experiment" is illustrated in Figure 4-36. The diameter of the hole is Ø 200 mm and the length will be at least 2 m. Water will be injected over the whole fracture plane with the same pressure at the same time as the water flow rates will be monitored in 5 cm sections, individual sections for left and right side. When injecting water with the same pressure over the whole

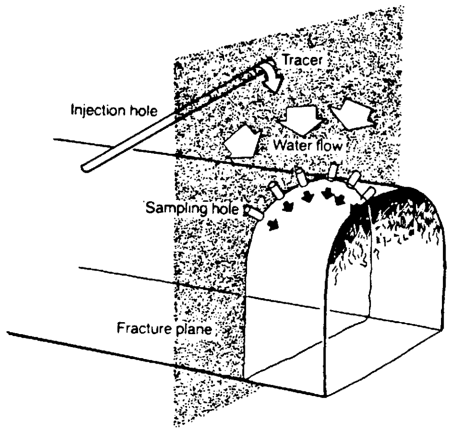

Figure 4-35. Layout of the "Migration in a Single Fracture" experiment, Stripa Project, Phase 1.

fracture plane there should not be any problems with pressure gradients between different channels.

A double hole experiment will be performed in order to investigate the fracture plane between the holes. The experimental layout of the double hole experiment is illustrated in Figure 4-37. The distance between the 2 holes will be about 2 m. Pressure tests as well as tracer tests will be performed between the holes.

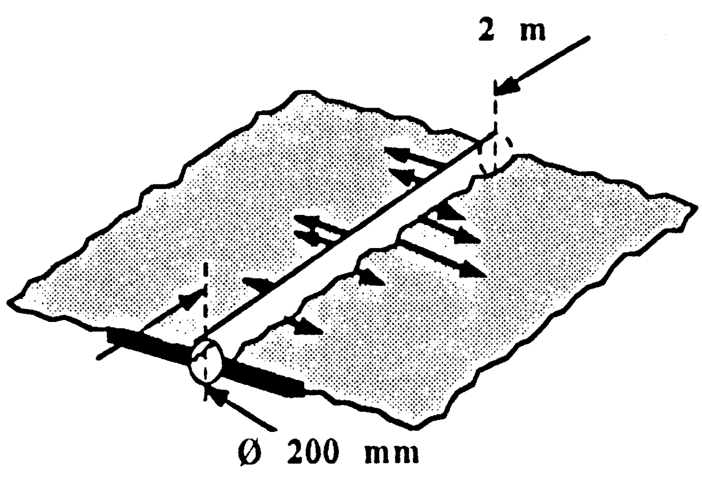

Figure 4-36. Layout of the single hole experiment.

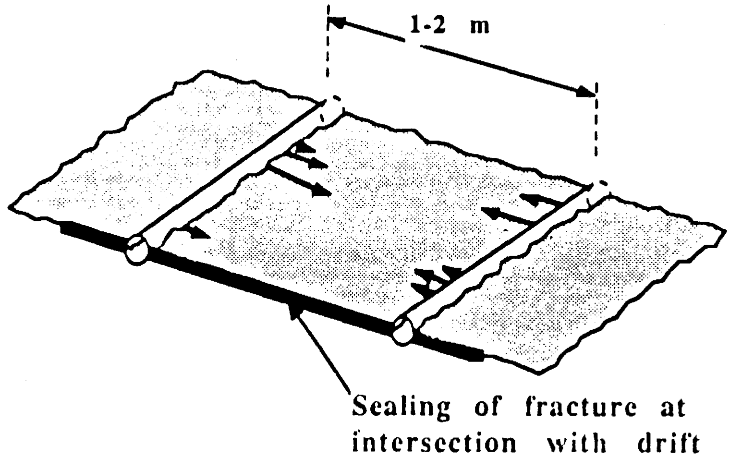

Figure 4-37. Layout of the double hole experiment.

4.5.4 Fracture Mapping

The single hole experiment as well as the double hole experiment requires fractures that are more or less planar at least 2 m into the rock. Therefore, a mapping of the most prominent fractures at the 360 m level has been done. This rough mapping gave about 100 fractures that might be suitable for the experiments. Laboratory and field experiments have showed that the hydraulic conductivity is almost independent of normal stress as long as the normal stress over the fracture plane is above about 3–4 MPa. Due to that criteria a more careful determination of the orientations and strikes of the mapped fractures has been performed in cooperation with VIAK AB, Falun, Sweden. The normal stress over each fracture plane has then been estimated using data from rock stress measurements performed at different locations in the mine. The major fracture characteristics of interest are:

- o fracture orientation,
- o fracture undulation,
- o rock type,
- o fracture filling,
- o evidence of water flow,
- o distances to other major fractures,
- o coarse estimate of normal stress over fracture plane.

4.5.5 Equipment

The equipment for the channelling experiments can be divided into three major parts, namely:

- o Packer system in injection hole.
- o Water injection system with flowmeters.
- o Data acquisition system.

The packer system consists of a outer packer which seals of the injection from the drift and a inner packer which has 40 rubber cups, 20 on each side, which can be individually adjusted to fit over the fracture intersection. Each rubber cup has its own piston by which it is pressed toward the wall of the borehole. By moving the packer system and switching which cups to monitor individually, the injection flow rates over 5 cm section along the whole intersection of the fracture plane with the large diameter hole can be monitored both on the left and right side. The packer system has a total length of 2.5 m of which 2 m is used for the actual measurements. The weight is approximately 100 kg. To facilitate the individual positioning of the rubber cups, the drill core will be put in a plexiglass cylinder, which is cut in two pieces along its axis, on which the fracture will be marked. The packer can then be put in the cylinder and the rubber cups adjusted.

The water is injected with a constant over-pressure obtained by compressed nitrogen. If necessary individual injection pressures can be set for 20 selected rubber cups. The injection flow rates are monitored in three groups, (1) the water flow which enters the uncovered part of the intersected fracture, (2) the sum of the water flow to 20 of the rubber cups, (3) the individual injection flow rates to the other 20 rubber cups. Injection flow rates of type (1) and (2) are monitored by precision balances. The individual injection flow rates into the rubber cups is monitored using a differential pressure transducer which registers the emptying of a vertical measuring tube. The flow monitoring system is flexible in such a way that the tubes are interchangeable and tubes of different diameters can be used to accommodate for a large range of flowrates. The measuring tube is automatically refilled when a preset low level is reached. 20 cups out of the 40 are equipped with such a measuring device. The injection system is designed for injection pressures up to 0.5 MPa. Preliminary tests show that injection flow rates down to a few hundreds of a milliliter per hour can be monitored.

Time, total injection pressures as well as the changes in the differential pressures are registered and stored on magnetic disks. During start-up and ending of a test settings of all the essential valves and diameters of the tubes as well as total water volume are automatically registered and stored on magnetic disks.

4.5.6 Time Schedule

The experiment started early this year and will continue until mid 1989. During 1987 the major part of the equipment was put together and tested in the laboratory. Some problems occurred with leakage due to defect solenoid valves. The first single hole test is planned to be performed in March 1988. The experiment is within the time schedule.

4.5.7 Discussion

Tests done in the laboratory indicate that the flow monitoring method using differential pressure transducers seems to be a good method for measuring very small injection flowrates.

4.6 ESTIMATION OF FRACTURE LENGTH AND APERTURE FROM SINGLE FRACTURE WELL TESTS

4.6.1 General

The objectives of the experiment are to obtain information on the length and interconnection of fractures from well tests performed in the Phase 3 study area. The tests are run using constant pressure methods while recording the transient flow rate. Additional tests are being performed to assess the effects of non-linear flow on well-test response curves.

4.6.2 Background

The network modelling approach requires information on the fracture system geometry and the transmissivity distribution of individual fractures. Presently, fracture geometric information is obtained by mapping fractures in core and on exposed surfaces. Mapping data does not reflect necessarily the hydraulic extent of the fractures, which may be less than the mappable length of the fracture.

The purpose of this project is use single fracture well tests to determine the hydraulic length and transmissivity (or aperture) of fractures. We are concentrating on the constant-pressure injection test for several reasons. The constant-pressure test (also known as the Lugeon test or packer test) has been widely applied to low-permeability, crystalline rock. Constant pressure tests have been the basic test used in the Swedish site characterization program (Almén, et al., 1986). The test has a major advantage over constant-rate methods in the absence of wellbore storage effects. Boundary effects are somewhat more distinctive in constant-pressure tests than in pulse or slug tests.

Hydraulic lengths of fractures are determined simply from indications of boundary effects in the constant-pressure tests. In sparsely fractured rock, such as that desired for waste repositories, single fractures may be viewed as individual, confined aquifers which may have a variety of geometries depending on their intersections with other fractures. The boundary effects are fundamentally of two types – open (or constant pressure) boundaries which reflect interconnection of fractures to more conductive features, and closed (or no-flow) boundaries which reflect termination of the fracture in solid, impermeable rock. The open boundaries are indicated by steady flow; closed boundaries are indicated by a flow rate that diminishes to zero as the boundary has its effect (Figure 4-38).

An additional task within this project has been to estimate the parameters of fracture spacing and aperture (or transmissivity) distributions from the properties of the cumula-

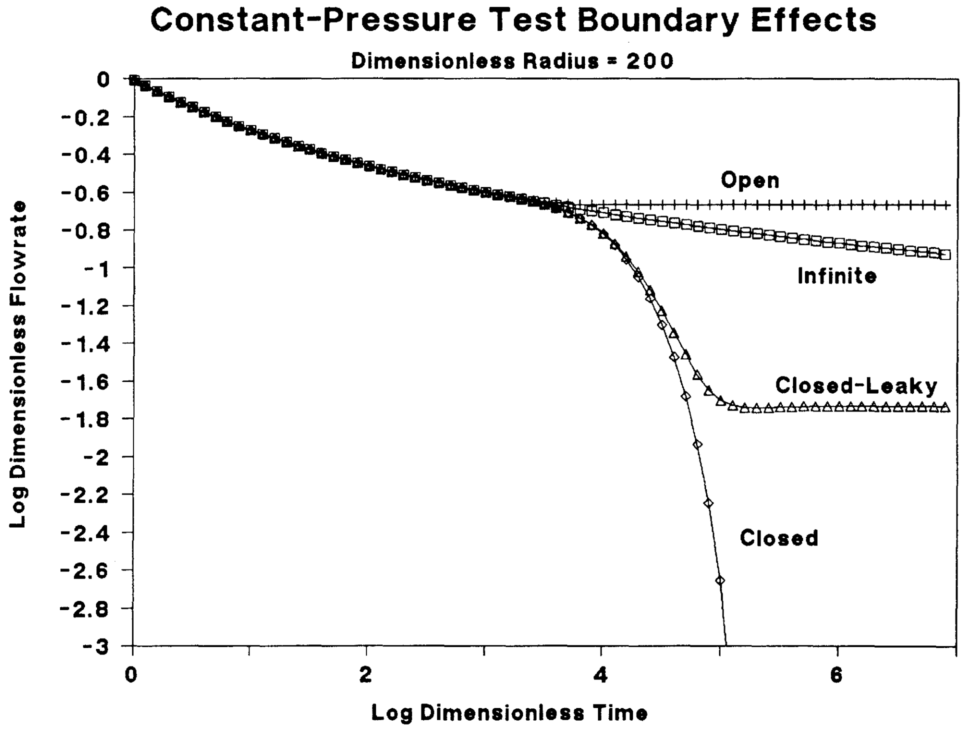

Figure 4-38. Example of type curve showing boundary effects for constant-pressure tests.

tive distribution of hydraulic conductivity values from a program of equally-spaced well tests. This approach was originally suggested by Snow (1970) and extended by Osnes (Doe, et al., in press). Tests using the multiplepacker system of developed by BGS and SGAB for use in the Phase 3 holes provides such as data base. The estimation of spacing and transmissivity distributions will be performed in 1988.

4.6.3 Progress in 1987 – Interpretation Methods

The project's activities in 1987 have been (1) to further develop solutions for constant-pressure well tests including leakage effects and a greater range of flow geometries and (2) to work with the British Geological Survey in performing constant pressure tests for determining boundary effects.

Specifically, we have prepared solutions for linear as well as radial flow solutions for constant-pressure test interpretation. The recognition of linear-versus radial-flow geometries is very important for assessing the influence of channelling. Linear flow should occur in well tests where the fractures are coaxial with respect to the borehole (for example, a vertical fracture in a vertical borehole) or where the flow in the fracture is restricted to one-dimensional channels.

A strong indication that channel flow occurs would come from identifying linear flow in fractures that are perpendicular to the borehole. Such fractures would be expected to sustain radial flow if the flow were distributed uniformly over the fracture's surface.

The solutions for analysis of constant-pressure test data have been compiled in a PC-based code, CH-QP, which will generate either type curves or specific curves for a range of conditions including leakage over the fracture face, finite fracture extent, closed boundaries, open boundaries (fracture interconnection), and skin effects. The code draws on analytical solutions for constant-pressure tests of Ehlig-Economides (1979) and storative leakage in manner analogous to Moench's (1985) approach for constant rate tests. The codes uses LaPlace transform space solutions which are inverted numerically. An example of open boundary and closed boundary type curves is shown in Figure 4-38. Copies of the code will be available as part of our final report to be produced during 1988.

To expand the potential data base for interpreting boundary effects, we have considered boundary effects in pulse and slug tests. During the past year we have developed curves for boundary effects in slug and pulse tests similar to those of Karasaki, 1986. Examples of slug and pulse curves with boundary effects are shown in Figure 4-39. Open boundary behavior results in a steepening of the pressure decay with respect to an infinite aquifer solution. Analysis of test data showing open boundary effects using infinite aquifer type curves does not result in significant transmissivity interpretation errors, however, it can yield abnormally low storage values. Closed boundaries are indicated by stabilization of the pressure pulse at a pressure higher (or lower in the case of pulse.slug withdrawal) than the initial test pressure. Preliminary review of data from the pulse testing program has not shown any indications of closed-boundary behavior, however, numerous zones have shown abnormally low storage values which may reflect open boundary behavior have been identified.

4.6.4 Field Testing in 1987

In selecting test zones, we have concentrated on zones which might show boundary effects. We have used several criteria. First, we have concentrated on high conductivity zones. We will be performing long term tests to determine the extent of high conductivity zones. We will also be performing multiple pressure tests to identify possible non-linear flow effects in these zones.

The second group of zones will be low-conductivity fractures near fracture zones. Such fractures should have a high likelihood of intersecting the fracture zones and thus exhibiting open-boundary behavior.

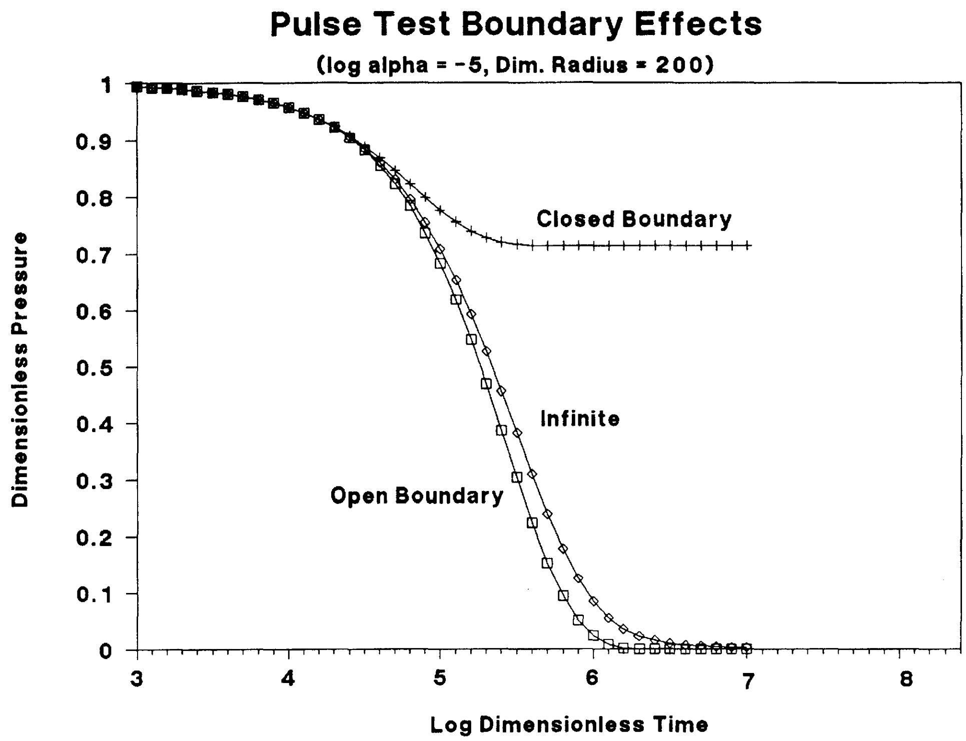

Figure 4-39. Type curves for pulse and slug tests showing effects of open and closed boundaries.

The third group of zones selected will be tests zones that show indications of boundary behavior in the pulse and slug tests that have been performed as part of the basic hydrologic characterization of the Phase 3 block. Preliminary review of pulse and slug test data has not found evidence for closed boundary conditions, however, numerous tests show the anomalously low storage values one would associate with open boundaries, as discussed in the previous section.

A first set of tests for boundary effects was performed in N4 in October, 1987. Initially, there were difficulties (1) in maintaining constant-pressure conditions in all but the highest conductivity zones and (2) in measuring low flowrates. The difficulties were overcome by adding a lower range flow meter to the BGS/SGAB test system and adopting procedures for constant pressure injection that use the slug test line as a static-pressure source for low permeability zones. These solutions have assured acquisition of high quality test data. The major portion of constant pressure tests for boundary effects are being performed in the "W"-holes in the first quarter of 1988.

4.7 ROCK SEALING

4.7.1 General

The object of the rock sealing project, in its first phase, is to identify suitable grouting materials and techniques to bring them into narrow fractures. A literature survey and state-of-the-art review of the function and longevity of grouts have been made, which indicated that smectite-based and cementitious grout materials are the most promising ones. Two major candidates have been investigated with respect to all major properties that control their groutability and longevity.

An earlier tested grouting technique based on superposition of static injection pressure and vibrations has been further developed.

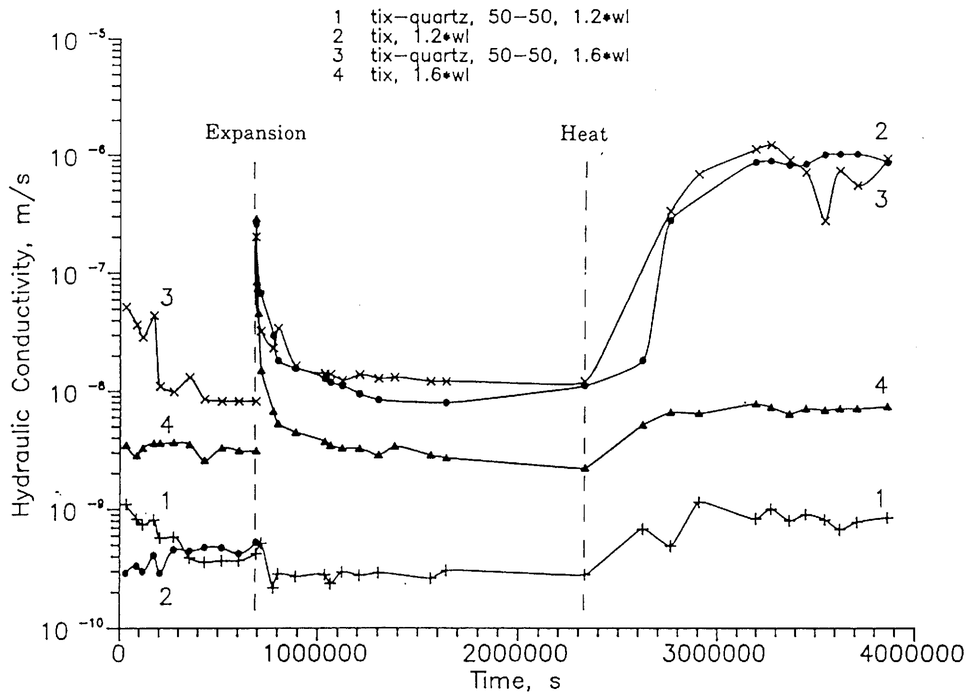

Figure 4-40. The hydraulic conductivity of four clay-based grouts as a function of fracture expansion by 30%, and heating to 90°C.

4.7.2 Physical Properties of Grouts

Two major grout materials have found to be the most promising candidate materials, i.e. finely ground cement with 10% silica fume and 1% superplasticizer (w/c ~0.4), and 50/50 Na bentonite and finely ground quartz powder. Their hydraulic conductivity appears to be sufficiently low to yield a net hydraulic conductivity of grouted rock of less than 10^{-10} m/s and they offer reasonably high resistance to piping and erosion. Lab percolation tests simulating widening of a sealed fracture by 10 – 30% at 90°C show that the conductivity of the expanded system is significantly increased, but that it is still not higher than 10^{-6} m/s (Figure 4-40), which still allows for a much lower net conductivity of the sealed rock. It is clear that there are options, a major one being clay/brine, which has a higher fluidity at a liquid content of 1.5 times the liquid limit and which is expected to consolidate very quickly in the rock, yielding a fresh- or brackish-water smectite with a density of about 1.3 t/m^3 and a very significant resistance to percolation, piping and erosion. The salt will diffuse very rapidly into the rock crystal matrix and leave an insignificant amount of dissolved NaCl in the porewater.

4.7.3 Longevity

The matter of longevity of the candidate grouts has been investigated but needs more attention. However, a preliminary estimate is that the chemical stability may be extremely long-lasting, i.e. tens or hundreds of thousand years depending on the temperature and percolation rates. Thus, it is felt that there is a very good basis for continuing the Stripa sealing project.

Among the most important findings is the one that soft Na montmorillonite clay gels may be much less sensitive to illitization than dense clay of the same type and that 130 – 150°C may be a critical temperature for the transformation to beidellite, which is a necessary prerequisite for conversion to illite. As to the cements, it seems as if salt water and low permeation would imply lifetimes exceeding tens or hundreds of thousand years.

A most important observation is that cement has a self-healing ability on mechanical fracturing and heating. This is due to a preserved hydration potential even at relatively high water contents.

4.7.4 Grouting Technique

The most essential goal of the Rock Sealing Project, i.e. to develop a technique to bring in grout into fractures with a "hydraulic" aperture of about 100 μm, has been reached. Actually, it has been demonstrated that clay and cement grouts of considerable density penetrate fractures with an aperture of down to 10 – 20 μm by applying the "Dynamic Injection Technique". The distribution of grouts in fractures can be reasonably well predicted on the basis of Lugeon testing and fracture mapping, applying a flow model that has been developed in the course of the project. This theory requires application of suitable flow parameters that depend on the grout density, the applied frequency, and the geometry of the system (fracture aperture, borehole diameter). Parameter values can be deduced from viscometer tests with special respect to the influence of vibrations.

4.7.5 Planned Work

The very promising laboratory and initial field tests strongly suggest continuation of the project. A Pilot Field Test has been planned to take place in early 1988, comprising Lugeon tests for hydraulic characterization of the test rock area and for prediction of the grout penetration. The test will have the form of grouting four 1.5 m long holes, two 7 m long ones and two 40 m long holes for checking the sealing effect and the agreement between predicted and actual distributions of the grouts in fractures that intersect the holes. The location of the grouts in the fractures will be documented through comprehensive excavation of the rock mass. Both cement and clay will be used.

4.8 ECONOMY

The total cost of the Stripa Project Phase 3 as of December 31, 1987 is given in the Table 4-4 below.

Table 4-4. Stripa Project Phase 3 – Summary of costs as per December 31, 1987. All figures in SEK.

Program	Original budget incl annual index esc. Jan 1988	Total program Accumulated	Total program Estimated Remaining
Project management	6 800 000	370 828	6 429 172
Stripa Generally	23 500 000	3 413 758	20 086 242
Site Char. and Validation	41 100 000	7 696 953	33 403 047
Dev. of Radar	5 200 000	2 452 861	2 747 139
Improv. of Bore-hole Seismics	3 400 000	711 917	2 688 083
Network Modelling	6 800 000	261 292	6 538 708
Channeling Experim.	7 000 000	2 186 433	4 813 567
Frac. length and Apert. f. Single	900 000	165 267	734 733
Sealing of Frac-tured Rock	7 500 000	3 883 866	3 616 134
Other Investi-gations	22 800 000	0	22 800 000
Total	**125 000 000**	**21 143 175**	**103 856 825**